chemosensors

MDPI

Review

Electrochemical vs. Optical Biosensors for Point-of-Care Applications: A Critical Review

Seyedeh Rojin Shariati Pour [1], Donato Calabria [2,3], Afsaneh Emamiamin [1], Elisa Lazzarini [2], Andrea Pace [2], Massimo Guardigli [2,3,4], Martina Zangheri [1,5,6,*] and Mara Mirasoli [1,3,4,*]

1 Department of Chemistry "Giacomo Ciamician", Alma Mater Studiorum, University of Bologna, Tecnopolo di Rimini, Via Dario Campana 71, I-47922 Rimini, Italy; seyedeh.shariatipou3@unibo.it (S.R.S.P.); afsaneh.emamiamin@studio.unibo.it (A.E.)
2 Department of Chemistry "Giacomo Ciamician", Alma Mater Studiorum, University of Bologna, Via Francesco Selmi 2, I-40126 Bologna, Italy; donato.calabria2@unibo.it (D.C.); elisa.lazzarini6@unibo.it (E.L.); andrea.pace7@unibo.it (A.P.); massimo.guardigli@unibo.it (M.G.)
3 Interdepartmental Centre for Industrial Aerospace Research (CIRI AEROSPACE), Alma Mater Studiorum, University of Bologna, Via Baldassarre Canaccini 12, I-47121 Forlì, Italy
4 Interdepartmental Centre for Industrial Research in Renewable Resources, Environment, Sea, and Energy (CIRI FRAME), Alma Mater Studiorum, University of Bologna, Via Sant'Alberto 163, I-48123 Ravenna, Italy
5 Interdepartmental Centre for Industrial Agrofood Research (CIRI AGRO), Alma Mater Studiorum, University of Bologna, Via Quinto Bucci 336, I-47521 Cesena, Italy
6 Interdepartmental Centre for Industrial Research in Advanced Mechanical Engineering Applications and Materials Technology (CIRI MAM), Alma Mater Studiorum, University of Bologna, Viale Risorgimento 2, I-40136 Bologna, Italy
* Correspondence: martina.zangheri2@unibo.it (M.Z.); mara.mirasoli@unibo.it (M.M.); Tel.: +39-0512099533 (M.M.)

Abstract: Analytical chemistry applied to medical and diagnostic analysis has recently focused on the development of cost-effective biosensors able to monitor the health status or to assess the level of specific biomarkers that can be indicative of several diseases. The improvement of technologies relating to the possibility of the non-invasive sampling of biological fluids, as well as sensors for the detection of analytical signals and the computational capabilities of the systems routinely employed in everyday life (e.g., smartphones, computers, etc.), makes the complete integration of self-standing analytical devices more accessible. This review aims to discuss the biosensors that have been proposed in the last five years focusing on two principal detecting approaches, optical and electrochemical, which have been employed for quantifying different kinds of target analytes reaching detection limits below the clinical sample levels required. These detection principles applied to point-of-care (POC) devices have been extensively reported in literature, and even the limited examples found on the market are based on these strategies. This work will show the latest innovations considering the integration of optical and electrochemical detection with the most commonly reported analytical platforms for POC applications such as paper-based or wearable and implantable devices.

Keywords: biosensor; electrochemical detection; optical detection; point-of-care; lab-on-chip; microfluidic device; paper-based device

Citation: Pour, S.R.S.; Calabria, D.; Emamiamin, A.; Lazzarini, E.; Pace, A.; Guardigli, M.; Zangheri, M.; Mirasoli, M. Electrochemical vs. Optical Biosensors for Point-of-Care Applications: A Critical Review. *Chemosensors* **2023**, *11*, 546. https://doi.org/10.3390/chemosensors11100546

Academic Editor: Alina Vasilescu

Received: 20 July 2023
Revised: 20 September 2023
Accepted: 7 October 2023
Published: 21 October 2023

1. Introduction

New technologies for the development of portable and self-standing devices for the rapid diagnosis of health disorders are emerging every day and they are linked to advances in different areas including chemistry, bioengineering, physics, and medicine. Indeed, the latest generation of biosensors has benefited from an interdisciplinary approach that has allowed the development of sophisticated and innovative analytical systems that could potentially improve human health, particularly in the developing world. In this context, the

point-of-care testing (POCT) approach represents a set of diagnostics that can allow us to detect rapidly diseases at the onset stage, leading to the execution of the suitable treatments. The International Organization for Standardization (ISO) qualifies POCT as 'testing that is performed near or at the site of a patient with the result leading to possible change in the care of the patient' [1]. Nowadays, POCT is used in very different settings, including general medicine, nursing, pharmacies, and on-site patient care [2]. The aim of POCT is to use the information obtained to apply, in a timely manner, the proper treatment [3] and to enlarge the accessibility to clinical diagnostics regardless of the existing medical and laboratory infrastructure [3–6]. Several POCT devices were proposed for different applications, such as the detection of bacteria [7–9], viruses [10–13], and biomarkers related to specific diseases or health conditions [14–17]. Their increased diffusion is partly due to technological advances that have made them more robust, easy-to-use, and cost-effective. Smartphone-based technologies, as well as lab-on-a-chip platforms and innovative assay formats, and advances in the long-term storage of reagents are also important factors that are decisive for the success of a POCT approach [4]. Indeed, these devices are based on biosensors able to combine in a unique platform bioanalytical assays and transduction systems for the acquisition and elaboration of analytical signals (Figure 1). The integrated platform should provide all the analytical steps, from the pretreatment of the sample, to the analysis and data processing stage, in order to obtain a qualitative and/or quantitative information. In light of these considerations, it is important that the optimization of the analytical assay, which should be based on the use of small volumes of the sample and reagents and on simple procedures, is accompanied by the development of portable and easy-to-use detectors.

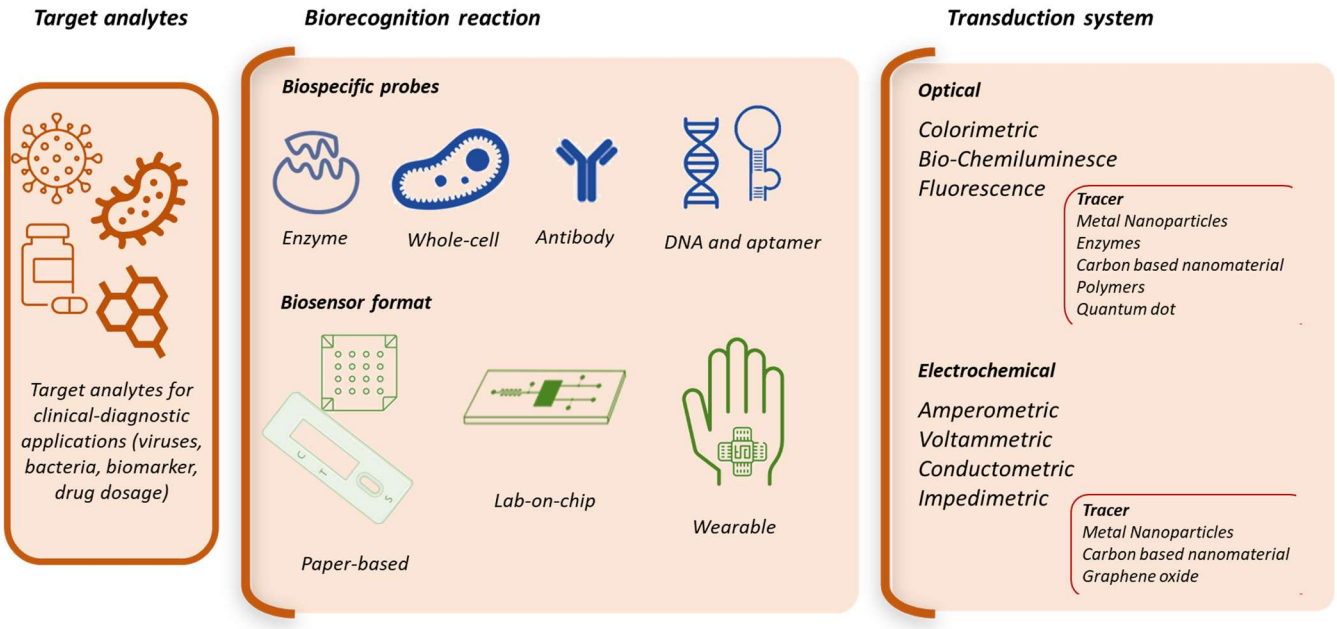

Figure 1. Scheme of the POCT devices considering the target analytes of interest, the biorecognition reactions, and the transduction systems that are most widely employed and can be selected depending on the needed performances and instrumental requirements of the analytical method.

As it concerns bioanalytical assays, the most widespread are those based on immunoassays. Indeed, the high specificity and selectivity make them ideal candidates for detecting low traces of target analytes even in complex matrices and small volumes. In the same way, enzymatic assays, already well-established in laboratory practice, have been extensively proposed for POCT platforms. Several devices actually spread on the market for clinical diagnostic purposes are based on these biorecognition reaction principles [18]. Recently, biosensors based on DNA or aptamer probes, as well as whole cell biosensors, are

also gaining interest among the scientific community. These innovative systems are very promising, taking advantage of their implementation with new nanomaterials, but, until now, their use has been limited to academic literature and they are not well established in the market [19,20]. Detection techniques combined with these bioassays and exploited for developing POCT devices are generally based on optical and electrochemical principles [18,21–24]. Optical biosensors can exploit different phenomena, depending on the tracer employed in the bioanalytical assay. One of the most widespread approach well-known for routinary applications is based on the use of metal nanoparticles (MNPs) which are present in strong surface plasmon resonance (SPR) bands, whose frequency can be tuned depending on the size and shape of the NP and on the nature of the metal, as well as on the composition of the surrounding environment [25]. This phenomenon is widely exploited by commercially available lateral flow immunoassays (LFIAs) which are well-known for their application in pregnancy tests and, more recently, for SARS-CoV-2 diagnosis. The LFIA is one of the most widespread colorimetric assay due to its simplicity, rapidity, cost-effectiveness, and lack of a requirement for equipment or required expertise for operation. This technique exploits immunoassays in which the sample and a labeled probe flow due to capillary forces along a porous membrane that contains immobilized biospecific reagents. These are placed in specific areas of the membrane, called Test and Control lines, where we can obtain information about the target analyte, and, simultaneously, we can assess the correct functioning of the test. The immunoreactions lead to the development of detectable colored bands that can be seen with the naked eye, corresponding to the Test and Control lines, due to the accumulation of the label in these areas which allow us to obtain qualitative information about the presence or the absence of the target analyte [26]. In this context, as in conventional colorimetric LFIAs, exploiting a Raman-reporter-labeled surface-enhanced Raman spectroscopy (SERS) conjugate, it is possible to assess the presence of the target analyte through a color change, but, additionally, quantitative information can be obtained by measuring the intensity of a characteristic Raman peak of reporter molecules. Raman equipment can be easily miniaturized and combined with portable formats for on-site, POC diagnostics of infectious diseases [27,28]. Indeed, several SERS-based analytical devices have been proposed for the rapid diagnostics of several diseases [29,30].

Otherwise, chemiluminescence (CL) is another optical technique alternative to the colorimetric approach and it is triggered by the passage of an atom or a molecule from an excited state to a steady state with the release of photons as a by-product of the chemical reaction [31]. CL-based biosensors usually rely on the use of enzymatic tracers that are able to catalyze CL reactions in the presence of a suitable substrate. The measurement of the produced photons can be related to the concentration of the target analyte, enabling a quantitative analysis, but it implies the use of an external detector able to detect luminescent signals. Nowadays, there is a wide range of choices of miniaturized and compact CL detectors that can be implemented into portable and easy-to-use analytical devices, since the main requisite is the ability to collect as much light as possible for achieving the highest detectability [32]. Besides the traditional photomultiplier, silicon p-i-n photodiodes have been extensively proposed since they guarantee a small size and low noise, together with a fast response time [33–35]. In addition, if it is necessary to obtain spatial information, the charge-coupled device (CCD) [36,37] and complementary metal-oxide semiconductor (CMOS) can be exploited for developing compact imaging systems. In particular, the use of the CMOS is attracting great attention since this technology is integrated into the smartphone photocamera, enabling the smartphone to be used as a portable CL detector [38–40]. In the context of CL detection, recently, the thermo-chemiluminescent (TCL) approach was also proposed, in which light emission is triggered by heating [41]. Therefore, the same instrumentation for acquiring photon emissions, with the addition of a heating system, is required to induce the luminescent phenomenon. As an optical transducing system, fluorescence (FL) has also been extensively proposed for developing clinical diagnostic biosensors due to its high sensitivity. In this case, however, the analytical device must be integrated with both the luminescent detector and a light source for exciting the fluorophore used as a label for the bioassay [42]. Another problem

in exploiting FL for biosensing is that the presence of some molecules (i.e., hemoglobin) can limit the possibility of exploiting this detection method. Therefore, as an alternative, the NIR wavelength has been recently proposed due to its higher transparency in biological fluid. In this region, the problem of autofluorescence is limited and the background signals are lower. Currently, NIR fluorophores show disadvantages like low quantum yield and low photostability, causing a limitation in their diffusion. On the other hand, electrochemical transducers usually are based on the measurement of the current developed during a redox reaction (amperometric and potentiometric methods) or of the change in surface conductivity and impedance (conductometric and impedimetric methods) [43]. Amperometric-based transducers are one of the most frequently used and, in this case, the measured current results from the oxidation and reduction reactions of the electroactive species. Amperometric measurements are performed by exploiting the passage of the current of the working electrode, keeping the potential unchanged against the reference electrode through the sample. Alternatively, if the current is measured in the presence of a controlled changes of the potential, the method is named voltammetry. Among the most widespread amperometric sensors, the glucose meter is one of the major ones applied for routinary analysis for people who suffer from diabetes mellitus or hypoglycemia. The assay is started by depositing a drop of blood on test strips equipped with an electrode containing glucose oxidase or dehydrogenase. Glucose present in the sample is oxidized by the enzyme, which is regenerated by the presence of a mediator reagent generating an electric signal. The total charge passing through the electrode is related to the concentration of glucose in the sample that has reacted in the presence of the enzyme. In addition, potentiometric-based biosensors focus on redox processes, but, in this case, the potential difference between the working and reference electrode is measured by a voltammeter. Impedimetric methods rely on the measurements of electrical changes that occur after a biorecognition reaction on the surface of a modified electrode. In particular, electrochemical impedance spectroscopy (EIS) is widely applied in developing biosensors based on the interactions between the biological probe and the target analyte that are selectively adsorbed on a modified electrode surface [44]. This adsorption causes changes in the kinetics of the electron transfer between a redox species present in the solution and the electrode. Through the monitoring of the transferred charge resistance (Rct), it is possible to quantitatively determine the amount of target analyte bound at the electrode surface. Finally, conductimetry can also be exploited for developing biosensors. An ohmmeter is used for measuring the change in conductance between two metal electrodes at a certain distance from each other. The change of ionic content enables a conductance that can be measured by applying to the electrode an alternating current.. Generally, the change of ionic strength occurs as a result of an enzymatic reaction in the system, so this technique is employed for developing enzyme-based biosensors.

To combine the advantages of electrochemical and optical detection, electrochemiluminescence (ECL) has been proposed, which is very wide employed for analytical routinary applications in laboratory settings. ECL is triggered by an electrochemical stimulus on a specific molecule [45,46]. Compared with other optical methods, ECL provides higher control on emitted light, a low background signal, and high sensitivity, as well as a wide dynamic range and rapid measurement [47,48]. On the other hand, with respect to other electrochemical techniques, it is less sensitive to interferences and a simpler detector can be exploited [49]. These aspects make ECL particularly suited for the development of portable biosensing devices [50,51].

A common aspect of optical and electrochemical detection is the increased use of the smartphone as a tool integrated in the biosensing device. Most applications reported the use of smartphones as a platform for data collection, transmission, and data elaboration. Smartphone cameras have been exploited as a detector for the acquisition of the signal in an optical-based assay. In this context, the most important challenge remains the control of light conditions, which implies the use of mini-boxes that enable the shielding of ambient light and the reproducibility of the acquisition of the signals [52]. On the other hand,

electrochemical-based assays exploit smartphones as an interface with which to control the measurements performed by a potentiostat, and the data transmission can be carried out wirelessly using Bluetooth or near-field communication (NFC). This means that there is the need for an external device for measuring signals and that the smartphone is not the detector but only an interface for managing the data. Recently, modules to be integrated into the hardware of the smartphone have been proposed in order to transform the smartphone into an electrochemical detection system. However, since smartphones are becoming more and more thin, it is becoming very difficult to implement the hardware with additional power-consuming components [53].

This review aims to show the state of the art on the development of POC biosensors for clinical diagnosis purposes based on optical (focusing on colorimetric, chemiluminescent, and fluorescent approaches) and electrochemical detection. The review will focus on the major latest achievements in this field, showing the advantages and the weakness of the two different approaches, as well as the possibilities for future development with a critical comparison with the widespread and commercialized systems that are already available.

2. Lab-on-Chip-Based Biosensors

The expression lab-on-chip (LOC) refers to a technology based on the integration of fluidic, biosensing probes and measuring components (electrodes or optical apparatus) onto the same chip [54–59].

As it concerns electrochemical biosensors, the methods require a set of electrodes (working, reference, and counter electrodes), their respective connectors, a potentiostat for regulating the electric processes, and a laptop (or similar) to analyze the data [60]. The computer and potentiostat have been already replaced by portable and handheld wireless all-in-one devices which are suitable for the POCT approach [61–67]. Following this trend, electrodes are also moving to easy-to-use and low-cost platforms, such screen-printed electrodes (SPEs) that are developed by depositing or pasting a combination of layers onto a wide variety of flat substrates [68]. Electrochemical techniques combined with SPEs have proven to be an ideal candidate for replacing conventional benchtop equipment with affordable, rapid, and portable devices, thus offering versatility in terms of electrode design, materials, and compatibility with different applications [69]. For developing biosensors, the immobilization of the recognition element onto the electrode surface is generally required. The immobilization processes on SPEs include different approaches such as adsorption, covalent coupling, entrapment, or cross-linking for obtaining the formation of a self-assembled monolayer of biospecific probes [70–73]. Hu et al. proposed an electrochemical immunochip based on a MoS_2/poly (diallyldimethylammonium chloride) (PDDA) hybrid film produced via a layer-by-layer self-assembly method [74]. An electrochemical impedance system was developed for the detection of alpha-fetoprotein (AFP). The platform was obtained by integrating a three-electrode system in the micro-channel, including MoS_2/PDDA film modified with antibodies specific for binding AFP as the working electrode, Ag/AgCl wire as the reference electrode, and indium tin oxide (ITO) as the counter electrode. This approach allowed us to obtain a linear range of 0.1 ng/mL to 10 ng/mL and a detection limit down to 0.033 ng/mL. Timilsin et al. described multi-electrode sensor chips suitable for detecting several analytes in complex biological fluids based on the sandwich enzyme-linked immunosorbent assay (ELISA) method [75] (Figure 2a). On a functionalized electrode coated with immobilized capture antibodies, samples containing the antigen and a secondary biotinylated detection antibody were added. Upon incubation, the specific antigen is detected through the formation of a sandwich between the capture and biotinylated detection antibodies. Finally, streptavidin poly-horseradish peroxidase (spHRP) was added in order to bind the biotinylated detection antibody and the measurement step was performed, exploiting the TMB substrate which causes the production of an electroconductive product that precipitates and that can be measured by cyclic voltammetry. A multiplex sensor for the detection of free and total prostate-specific antigen was obtained on SPE surfaces for detecting the human chorionic gonadotropin hormone [76]. The authors

described an electrochemical-based immunoassay, based on the electrochemical activity of AuNPs on SPEs. The electrode surface was functionalized with a primary antibody and a non-competitive immunoassay was carried out. Then, a secondary antibody conjugated with Au NPs was employed by applying 1.2 V; the Au NPs changed their oxidation state from Au^0 to Au^{3+}. Differential pulse voltammetry (DPV) from 0 V to 1.0 V was performed after the pre-oxidation step, reducing the oxidized NPs back to Au^0. The reduction process can be measured at 0.48 V.

Electrochemical LOC devices have also been exhaustively proposed for the detection of viruses [77–82] and, recently, they have been applied for diagnosing SARS-CoV-2 [82] (Table 1). In Seo et al.'s study, functionalized graphene with the SARS-CoV-2 spike antibody and the detection of the virus were performed both in the transport medium and clinical sample with an LOD of 1 fg/mL [83]. Zhao et al. [84] proposed the use of calixarene-functionalized graphene oxide for detecting the RNA of SARS-CoV-2 without nucleic acid amplification by exploiting a portable electrochemical smartphone. The LOD of the clinical specimen was 200 copies/mL and only two copies (10 µL) of SARS-CoV-2 were required for starting the assay. Azahar et al. [85] reported on the development of 3D nanoprinted electrodes, coated by nanoflakes of reduced graphene oxide (rGO) functionalized with specific viral antigens (Figure 2b). The electrodes were implemented into a microfluidic device and used in a standard electrochemical cell. The antibodies present in the sample selectively bound the antigens, changing the impedance of the electrical circuit which was detected by a smartphone interface. Furthermore, the sensor can be reused by regenerating it within a minute by using a low-pH solution suitable for eluting the antigens, allowing the successive use of the same sensor.

As with electrochemical detection, optical detection also requires additional components that have to be integrated into the LOC device. Indeed, while electrochemistry needs the presence of electrodes and a potentiostat, optical equipment comprises a detector suitable for quantifying the colorimetric assay, and CL or FL signals (in the last case, an excitation source is also required for exciting the fluorescent specie). In an optics of integration with LOC devices, recently, several detectors that combine an adequate sensitivity with portability have been proposed for developing ultrasensitive POCT assays [32,86]. For example, optical biosensors were realized using a new generation of (thermally cooled) back-illuminated (BI) CCDs [36] and smartphone BI-CMOS cameras [40], or thin-film photosensors [87], or amorphous silicon (a-Si:H) photosensors [88]. Fluorescent detection has been widely proposed for the development of LOC devices. Dinter et al. [89] developed an adaptable platform to detect biomarkers using a microfluidic technology (Figure 2c). They were able to distinguish fluorescently labeled biomarkers exploiting an immunoassay based on physically and spectroscopically different functionalized microbeads. This multiplexing approach allowed us to quantify four cardiovascular disease biomarkers using a commercial video imaging detector. In addition, Chang et al. [90] proposed an FL immunoassay developing a 3D microfluidic chip composed by a nickel mesh that acted as a bead trap between two layers sealed together by an adhesive of the PET sheet. Photonic crystal beads (PCBs) functionalized with capture antibodies are blocked into the microfluidic chip entrapment, into the grid of the nickel mesh. FL immunoassays were performed in the microfluidic chip and the signals were acquired, exploiting an FL microscope equipped with a CCD. The PCBs were encoded by their colors coming from the photonic structure and the analysis of the target analytes (human immunoglobulin G, carcinoembryonic antigen, and alpha fetoprotein) were performed by identifying the PCB colors and quantifying the FL intensity. Another work based on FL detection was proposed by Yuan et al. [91] The authors proposed an assay for the detection of one of the four serotypes of the dengue virus non-structural protein (DENV-NS1) and its cognate human IgG. In this system, the FL microbeads are imaged through a microfluidic chip using a microscope system. To capture the dengue virus non-structural protein (DENV-NS1), the magnetic beads with a higher dye concentration were functionalized with the anti-DENV-NS1 antibody, while the beads with a lower dye concentration were coupled with DENV-NS1 to capture anti-DENV-NS1

antibodies. These beads were then introduced into the microfluidic chip for analysis using a portable imaging setup. These examples show the difficult integration between the LOC device and the detector for the measurement of analytical signals. Indeed, the detection system is generally benchtop instrumentation applied for acquiring FL signals that occur in a microfluidic chip. The implementation of LOC devices is better achieved in the field of CL. Dei et al. [92] developed a portable instrument for CL detection and signal elaboration. They proposed a microfluidic chip in which the flow started by capillary pumping and continued by the imbibition of a filter paper. Microfluidic units make possible the notion that the flow passes through the reaction areas at a reduced flux to enable the binding between the antigen and antibody, speeding up after the reaction areas. By immobilizing different antibodies into the reaction area, four types of biomarkers can be measured simultaneously. The system was tested by analyzing four biomarkers of colorectal cancer using plasma samples from patients. Sharafeldin et al. [93] combined a system of micropumps and an Arduino microcontroller to develop an automated 3D-printed device that lysed cells and performed a non-competitive immunoassay for the four biomarkers. The chip was composed of a detection chamber in which the inner walls coated with chitosan hydrogel film were functionalized with capture antibodies (Figure 2d). Non-competitive immunoassays were performed and the CL signals were acquired on a CCD camera. In addition to FL and CL, bioluminescence (BL) can also be exploited for the development of LOC devices. Mirasoli et al. [94] described an integrated lab-on-chip system, in which we see the amplification of viral DNA composed of a disposable polydimethylsiloxane (PDMS) reaction chamber (10-µL) coupled to a glass substrate in which a thin-film metallic resistive heater and (a-Si:H) photosensors which act as a light detector were integrated. A loop-mediated isothermal amplification (LAMP) technique was developed for specifically amplifying parvovirus B19 DNA and it was coupled with Bioluminescent Assay in Real Time (BART) technology for providing the real-time detection of the target DNA.

As an alternative, the ECL approach was employed by Calabria et al. [95] for developing a 3D-printed miniaturized biosensor for glucose detection. The system employed a two-electrode configuration and it relied on the glucose oxidation catalyzed by glucose oxidase. The developed hydrogen peroxide was detected by the addition of luminol and the ECL signal was acquired by employing a smartphone.

As has emerged from the reported works, the development of LOC devices has required, in recent years, a great effort mainly addressed at the resolution of problems such as the implementation of a bioassay on a microfluidic platform and the increase in the sensitivity of analytical methods (e.g., the use of nanomaterials, innovative tracers, and signal amplification). From this point of view, LOC biosensors have significantly improved their potential, reaching performances that are comparable with those obtained using laboratory settings. To date, the most critical aspect remains the complete integration of the microfluidic device with the signal detector. Indeed, many works report the development of miniaturized and easy-to-use microfluidic platforms, but the detection step is very often performed with benchtop instrumentation. From this point of view, the use of the smartphone (both for electrochemical and optical detection) represents a very important possibility for making these devices more usable even by non-specialized personnel. Instead, limited to optical detection, the use of low-cost photosensors is also a significant step forward in achieving the full integration of the analytical device.

In the case of LOC biosensors, electrochemical and optical approaches are promising. Indeed, from the point of view of operational simplicity, electrochemical detection is advantageous, as the necessary microfluidics are simplified by the fact that it is not necessary to add reagents contrary to what happens with optical detection methods. On the other hand, however, due to technological innovations, optical detectors achieve high degrees of integration with the analytical device, allowing high sensitivity to be combined with portability and low cost.

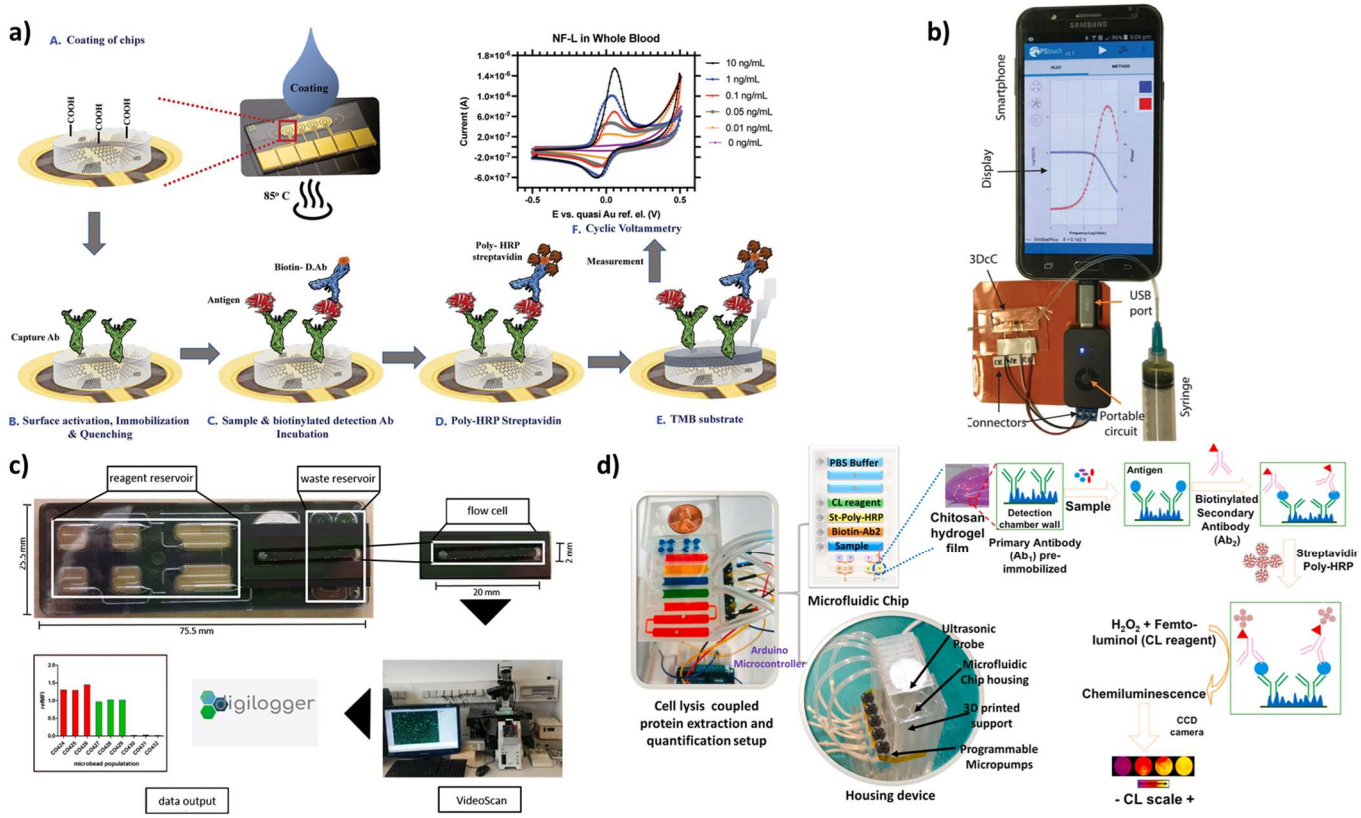

Figure 2. Scheme of working principle of the analytical device: (**a**) 3D schematic of sandwich immunoassay on biosensor coated with antifouling nanocomposite: A. Electrochemical sensor with gold electrodes; B. Immobilization of capture antibody and saturation with BSA; C. Incubation of sample mixed with biotinylated detection antibodies; D. Addition of poly-HRP streptavidin; E. Addition of TMB followed by precipitation over the gold electrode; F. Results of the cyclic voltammetry. Reprinted with permission from Ref. [75]; (**b**) The electrochemical analytical device interfaced with a portable potentiostat connected to a smartphone via a USB-C connection to measure the signal. Reprinted with permission from Ref. [85]; (**c**) Microbeads immobilized in microfluidic chip and reagent reservoirs filled with assay reagents. Pumps inject reagents during the assay. Measurements were performed using VideoScan technology (bioimage informatics). Reprinted with permission from Ref. [89]; (**d**) Device design comprising a microfluidic chip with 5 inlets connected to peristaltic micropumps, sample, and rectangular prism reagent chambers with capacity of 80 ± 5 µL, and 8 cylindrical detection chambers with 8 ± 1 µL capacity each. A microfluidic chip is designed to house sample and reagents and deliver them sequentially to detection compartment. The assay protocol is based on poly-HRP and ultra-bright femto-luminol to produce CL that is measured using a CCD camera. Reprinted with permission from Ref. [93].

3. Paper-Based Diagnostic Devices

Paper-based devices have represented a real revolution in do-it-yourself diagnostics and most of the biosensors currently on the market for POCT applications are based on this platform. In addition to accessibility, affordability, and ease of disposal compared to traditional materials used in microfluidics, paper is also suitable for being processed in many different ways including printing, coating, cutting, and lamination. This peculiarity offers a great versatility and the opportunity to design different devices that potentially can be mass-produced with low cost [96,97]. By changing the properties such as hydrophobicity, conductivity, porosity, and reactivity (modifying the chemical structure), paper could be adapted to a specific need [98]. Furthermore, the use of paper as the sensing element allows us to simplify the required instrumentation since the capillary force can drive fluid without an external pump.

Indeed, the most successfully commercialized devices with both electrochemical and optical detection are based on the use of paper as the analytical platform. Most glucometers, for example, are based on the use of disposable strips on which the reagents necessary for performing the test are immobilized. The detection is carried out by adding a drop of blood on the strip, and then inserting it into the portable detector. Since the introduction of the first prototype of the glucometer, many electrochemical biosensors have been proposed in literature, and, recently, some new nanomaterials have been proposed for increasing the analytical performances [99–107].

Similarly, the most common optical detection tests commercially available for POCT (pregnancy tests and COVID-19 tests) are also based on the LFIA technique. Traditionally, LFIAs are employed for qualitative analyses, which involved the user's conclusion about the presence or absence of a specific target analyte in the sample based on a visual evaluation of the colored bands formed upon the strip. Recently, this technique was implemented in order to obtain a quantitative output due to the combination with different detection principles [108]. Indeed, over the past decade, several affordable and compact detectors have been designed for integrating the LFIA strip with a portable and easy-to-use system [109–111]. Even if the inclusion of instrumental measurement can complicate the analytical procedure, the possibility of obtaining quantitative information for several biomarkers without the need for an equipped laboratory is attracting great attention [112]. In this context, optical detection can be performed, exploiting the quantification of analytical signals due to both color formation and photon emission. Concerning the colorimetric quantitative detection, the image analysis exploiting RGB or HSV data is the most exploited approach. In this system, the digital image that can also be taken with a smartphone's camera is elaborated with dedicated software (i.e., Image J), which can extract RGB color values from the image. The raw plot of RGB color values can be converted into a logarithmic scale and plotted against the concentration of the target analyte, following a Lambert–Beer law trend [113]. One of the applications on which more publications based on colorimetric LFIAs have been reported is about the detection of SARS-CoV-2 (Table 1). Indeed, from 2020, several analytical devices have been released in commerce for the diagnosis of this disease. Literature focuses on the possibility of improving the detectability of these systems. Lee et al. [114] developed a colorimetric LFIA exploiting a specific linker for immobilizing antibodies on the cellulose membrane in an oriented manner. The proposed system allowed us to increase the sensitivity with a detection limit of 5×10^4 copies/mL. Another approach for improving the performances of the method relied on the combination of different detection principles. For example, a colorimetric and FL LFIA biosensor was proposed for the detection of the spike 1 (S1) protein of SARS-CoV-2 by Han et al. [115]. The dual approach allowed us to combine a rapid visual detection for the screening of suspected SARS-CoV-2 infection on sites while the FL signal allowed the quantitative detection of virus infection at the early stage. The authors coated a single-layer shell formed by mixing 20 nm Au NP and quantum dots (QDs) on an SiO_2 core to produce a dual immune label that simultaneously produced strong colorimetric and fluorescence signals. The detection limits of detecting the S1 protein via the colorimetric and fluorescence functions of the biosensor were 1 and 0.033 ng/mL, respectively. Moreover, Roda et al. [116] proposed a dual optical/CL format of the LFIA immunosensor for IgA detection in serum and saliva, exploiting a recombinant nucleocapsid antigen which specifically captured SARS-CoV-2 antibodies in patient specimens. As the detection system, a smartphone-camera-based device measures the color signal provided by nanogold-labelled anti-human IgA, while, for the CL measurements, a CCD was employed for acquiring the light signal resulting from the reaction of the HRP-labelled anti-human IgA with a H_2O_2/luminol/enhancers substrate. The use of the smartphone has been widely proposed in the field of optical detection associated with the LFIA technique [117–119]. Li et al. [120] designed a QD LFIA for the FL detection of a specific IgG for SARS-CoV-2 in human serum or whole blood samples. In this case, the smartphone was employed as an interface for elaborating the FL signals; indeed, the detector was a portable fluorescence strip reader connected via Wi-Fi

to a smartphone platform. Mahmoud et al. [121] exploited the smartphone directly as an FL detector, by developing a 3D-printed smartphone imager with a built-in UV-LED light source. Interleukin-6 and thrombin were measured by using FL green and red QDs as labels for the two target analytes, respectively. Through the separation of RGB channels, the acquired images can be processed to simultaneously quantify two analytes on the same test line, enabling the optical multiplexing approach. Moreover, Rong et al. [122] developed a smartphone-based FL-LFIA platform for the detection of Zika virus non-structural protein 1 (ZIKV NS1), exploiting QD microspheres as FL probes. A device to be integrated with the smartphone, comprising optical and electrical components, was designed and 3D-printed (Figure 3a). The implementation of CL detection with the smartphone camera has been also investigated. Chabi et al. [123] reported an LFIA platform employing phage-based CL reporters, combined with smartphone detection and applied to the diagnosis of SARS-CoV-2. Exploiting the same approach, Ren et al. [124], trying to increase the sensitivity of the system, proposed a CL-LFIA based on the synthesis of the Au NP-antibody-HRP-polyethylene glyco conjugate for detecting cardiac troponin I (Figure 3b). Due to the presence of polyethylene glycol that allowed a controlled orientation of the immunocoplex, the accuracy of the LFIA was improved significantly, allowing a detection limit of 10 pg/mL. In the context of CL detection, Calabria et al. [33] employed an origami-paper-based analytical device (μPAD) format allowing the preloading of the reagents required in the dried form on the paper substrate. The analytical protocols were initiated by injecting a buffer solution on the μPAD, and the device was designed to be a part of the AstroBio CubeSat (ABCS) nanosatellite. This biosensor represented the first step in developing an innovative technology to conduct research in space, implementing different kinds of bioassays on the same platform to verify their compatibility with the effect of deep space conditions. An example of paper-based device was also proposed combined with TCL detection. Roda et al. [125] reported a TCL vertical flow immunoassay (VFIA) in which a one-step test was performed for detecting valproic acid. The VFIA sensor was composed of several layers functionalized with reagents stably stored and by 3D printing; accessories were produced to make a smartphone become a biosensing device that provides a power source for the heating process necessary to start the TCL reaction and a camera for measuring emitted photons.

As it concerns the electrochemical detection applied on paper-based devices, the electrode fabrication is a fundamental step for their development [126,127]. The first example was reported by Henry et al. [128], who proposed using carbon SPE on filter paper. From this pioneering work, several devices have been presented, based on different electrode fabrication techniques [129]. Moreover, LFIA has been extensively combined with electrochemical detection by implementing the nitrocellulose membrane with SPE. The main difference with the optical-based LFIA is that, in the electrochemical approach, the membrane presents only the test line equipped with the SPE. The labels selected are generally molecules that undergo an oxidation–reduction process on the electrode surface, or enzymes which can facilitate the oxidation–reduction reaction, producing an electrical current or changes in other electrical properties. A portable potentiometer is then employed in order to acquire the signal through the electrode for performing quantitative analysis [130]. Deenin et al. [131] proposed a biosensor for diagnosing COVID-19 based on a test strip integrated with an SPE (Figure 3c). The ferrocene carboxylic acid was used as a tracer for the SARS-CoV-2 antibody that binds the SARS-CoV-2 antigen in the sample before flowing on the strip. On the test line, corresponding with the electrode, the angiotensin-converting enzyme 2 (ACE2) receptor was immobilized for capturing the immunocomplex formed in the presence of the target analyte. The electrochemical signal was measured with a smartphone interface, achieving a detection limit of 2.98 pg/mL. Sinawang et al. [132] presented a work for the quantification of the dengue NS1 protein in human serum based on electroactive immunonanoparticles able to capture the target analyte and then move on a functionalized gold SPE electrode for producing an amperometric signal measured by a potentiostat (Figure 3d). The gold SPE worked simultaneously as a signal transducer

and a solid-state support for a sandwich ELISA-like immunoassay. Srisomwat et al. [133] proposed an automated electrochemical LFIA device for the quantitative detection of the hepatitis B virus (HBV). The novelty is related to the use of a time-delayed microfluidic strategy fabricated on paper, which allowed a sequenced solution transfer. The device consisted of a straight nondelayed channel, a zigzag delayed channel, and a detection zone. In this configuration, the high-performance pyrrolidinyl peptide nucleic acid (acpcPNA) probe was used for functionalizing the T-line of the test strip which comprised an electrode. The Au^{3+} for gold metallization was stored at the delayed channel area. When the sample containing the HBV DNA was added, the solution moved across the nondelayed channel hybridizing the acpcPNA probe at the T-line. The wax-printed barriers made the solution flow retarded in order to gradually merge the preceding flow coming from the nondelayed channel. Taking advantage of this difference, DNA hybridization occurred first, and then Au^{3+} bound the captured DNA. These steps were performed automatically and sequentially after the sample addition and the buffer flow without the need of additional steps.

Moreover, LFIA was combined with ECL detection. Tris(2,2′-bipyridyl)ruthenium (II) [Ru(bpy)32+], a photoactive species with optical properties, is frequently exploited in ECL-based sensing systems due to its solubility in water, high electrochemical stability, and since it enables the regeneration in ECL reactions in the presence of tripropylamine (TPA). Hong et al. [134] proposed an ECL-LFIA for detecting troponin using Ru(bpy)32+-loaded mesoporous silica nanoparticles (RMSNs). Antibody-immobilized RMSNs were used for developing a non-competitive LFIA and the detection was performed using a CCD camera.

The widespread diffusion of paper-based devices in commerce and in our everyday life demonstrates how this approach is functional and effective when combined with both electrochemical and optical detection. Certainly, in the future, qualitative detection technologies based on colorimetric detection could be replaced by more advanced quantitative systems which could give additional information and could, therefore, be applied to different types of target analytes, including specific biomarkers for the diagnosis or monitoring of several diseases. This will lead to an increasing interest in the research field in improving the implementation of detectors on entirely portable platforms and increasing the sensitivity of the analytical methods involved. In this context, both electrochemical detection methods and those based on CL and FL can represent a valid alternative to the traditionally used colorimetric methods. Moreover, in this case, the electrochemical approach offers the possibility of exploiting methods in which the addition of reagents is not necessary. Currently, however, even in the case of optical detection, paper-based systems increasingly involve the integration of all the reagents necessary for the development of the analytical signal directly on the membranes that constitute the device, guaranteeing a rapid and simple one-step analysis.

Table 1. Comparison between biosensing devices for the diagnosis of SARS-CoV-2.

Platform	Principle of Detection	Mechanism of Biosensing	Equipment	LOD	REF
Lab-on-chip	Electrochemical	SARS-CoV-2 spike antibody was immobilized onto graphene sheets that coated the biosensing device for the detection of SARS-CoV-2 spike protein.	Field-effect transistor (FET)-based device functionalized with SARS-CoV-2 spike antibody.	242 copies/mL	[83]

Table 1. *Cont.*

Platform	Principle of Detection	Mechanism of Biosensing	Equipment	LOD	REF
Lab-on-chip	Electrochemical	Calixarene-functionalized graphene oxide for detecting RNA of SARS-CoV-2 without nucleic acid amplification by exploiting a portable electrochemical smartphone.	A carbon, three-electrode screen-printed carbon electrode (SPCE) was employed as platform for differential pulse voltammetry, which was performed with a smartphone equipped with a Sensit Smart electrochemical workstation from Palmsens.	200 copies/mL	[84]
Lab-on-chip	Electrochemical	The detection of antibodies specific to SARS-CoV-2 was achieved, immobilizing antigens on the 3D gold micropillar array electrodes functionalized with rGO nanoflakes.	The electrode is integrated with a microfluidic device and used in a standard electrochemical cell, and the measurement was performed using a smartphone-based user interface.	2.8×10^{-15} (antibodies to SARS-CoV-2 spike S1 protein) and 16.9×10^{-15} M RBD	[85]
LFIA	Colorimetric	The test line contains a capture antibody with immobilized CBP31-BC to detect the SARS-CoV-2 spike antigen. CBP31-BC alone is used for the control line. For detection, SARS-CoV-2 spike antibody was conjugated to AuNPs	The qualitative detection can be carried out visually; for quantitative information, the images of the strip were acquired with a smartphone's camera and analyzed with a suitable software.	5×10^4 copies/mL	[114]
LFIA	Colorimetric and fluorescent	SARS-CoV-2 spike 1 capture antibody was immobilized on the T line, and, when the antigens were captured, a second detection antibody conjugated with SiO_2@Au/QD NPs was employed	For the colorimetric approach, visual detection was used, while, for the fluorescent quantitative measurement, a fluorescent strip reader was required.	1 ng/mL (colorimetric approach) and 0.033 ng/mL (fluorescent approach).	[115]

Table 1. *Cont.*

Platform	Principle of Detection	Mechanism of Biosensing	Equipment	LOD	REF
LFIA	Colorimetrich and chemilumi-nescent	The serum or salivary sample is applied to the sample and resuspends the probe (AuNP- or HRP-labelled anti-human IgA), and the mix flows through the detection membrane where it encounters the nucleocapsid protein on the test line and the staphylococcal protein A on the control line (CL). Anti-SARS-CoV-2 IgA in the sample is selectively captured at the test line.	For the (semi)-quantitative colorimetric evaluation, the LFIA strip was placed in front of the smartphone camera, inside the mini dark box to exclude ambient light, and an additional lens was used to focus the T and C line image and standardize the reading using the smartphone flash illumination. A semicover and a mini dark box adaptable to any smartphones were made with 3D printing. For the chemiluminescence detection, we developed a simple device based on a cooled CCD camera with the LFIA strip in contact with the sensor using a fiber-optic faceplate.	Not available.	[116]
LFIA	Chemiluminescent	SARS-CoV-2 nucleoprotein is sandwiched between mouse detection antibodies and rabbit capture antibodies on the LFA test line (TL) and then detected by anti-mouse antibody-HRP phage reporters.	A smartphone fitted with a 3D-printed lens-free accessory to properly position the strip directly under the back camera was used as CL detector. An in-house-developed iOS app was used for image analysis.	25 pg/mL nucleoprotein	[123]
LFIA	Electrochemical	The ferrocene carboxylic acid-SARS-CoV-2 antibody is the probe employed for capturing antigens as an immunocomplex. The ACE2 receptor immobilized on the electrode is responsible for capturing this immunocomplex, and the corresponding electrochemical signal produced is observed using a smartphone.	The screen-printed electrode was placed between the backing card and the nitrocellulose membrane of the LFIA strip. The device was packaged on cassette in order to be ready to use with the smartphone-based reader.	2.98 pg/mL spike antigen	[131]

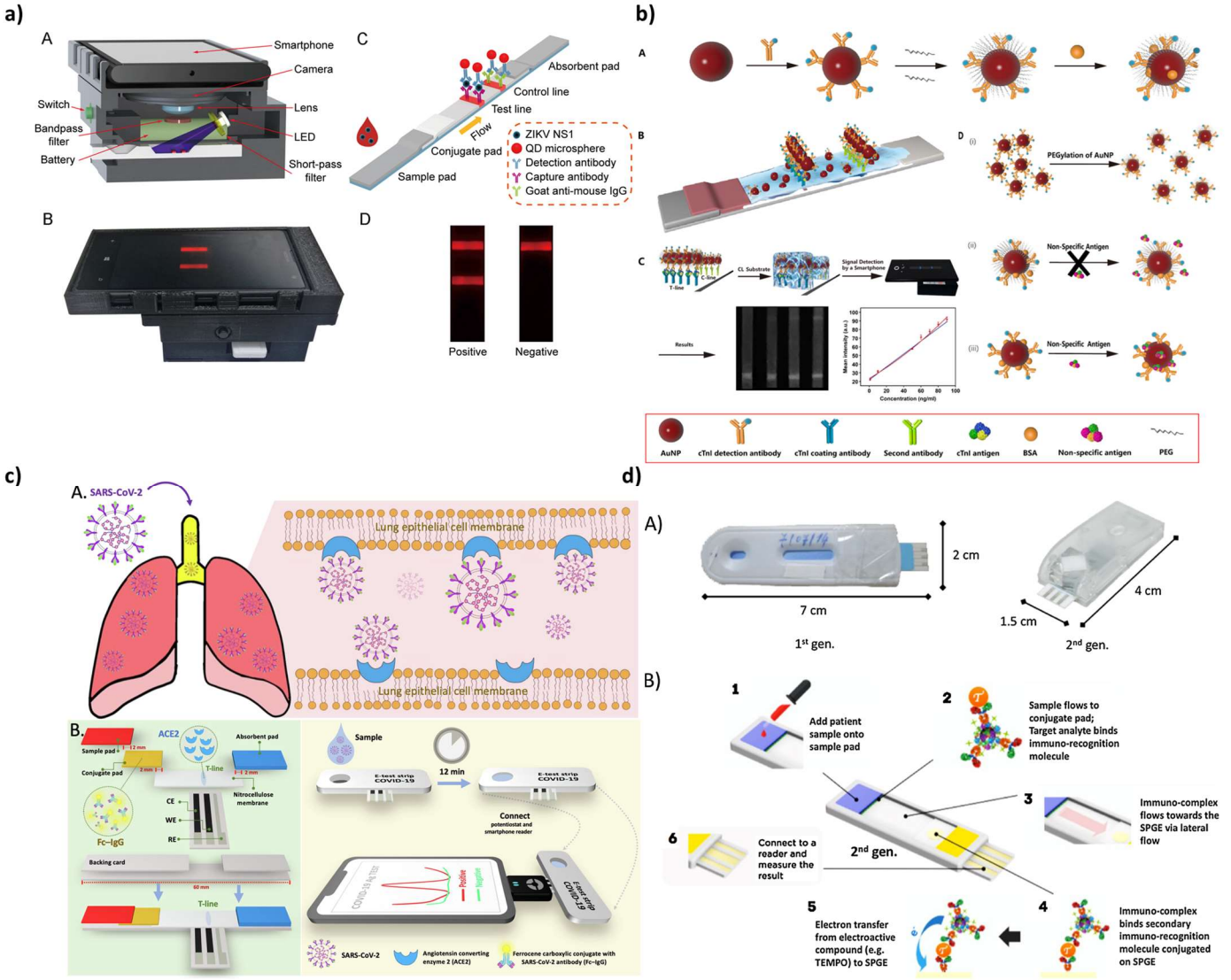

Figure 3. (**a**) Scheme of the design and application of the smartphone-based fluorescent LFIA platform: A. Internal structure of 3D smartphone-based imaging device; B: Photo of the developed fluorescent LFIA reader; C. Schematic of the fluorescent LFIA for the detection of ZIKV NS1; D. Images of the test strips in the presence (left) and absence (right) of ZIKV NS1. Reprinted with permission from Ref. [122]; (**b**) LFIA based on the PEGylation of AuNPs. A. Preparation of AuNP-Ab-HRP-PEG conjugates based on the PEG-modified AuNPs. The conjugates were prepared by the physisorption of antibodies, Au–S covalent bonding between AuNP and mPEG-SH and finally the physisorption of BSA, sequentially. B. Illustration of CL-LFIA based on applying the AuNP-Ab-HRP-PEG conjugates to the detection. C. Illustration of light signal detection with a camera of a cell phone and the results of cTnI detection. D. Illustration of the PEGylation of AuNPs for improving the performance of CL-LFIA biosensor. (i) Nonspecific adsorption of the AuNP-Ab conjugate without PEG. (ii) PEGylation diminished the nonspecific adsorption of AuNP. (iii) Aggregation of AuNPs can be solved by PEGylation, and thus, the solution becomes more dispersed. Reprinted with permission from [124], Copyright {2023} American Chemical Society; (**c**) Schematic illustration of the E-test strip testing: A. SARS-CoV-2 binding with the ACE2 cellular receptor; B. Schematic of the E-test strip in which the SARS-CoV-2 spike antigen is detected using the ACE2 WE test zone on the nitrocellulose membrane. Reprinted with permission from Ref. [131]; (**d**) A. Electrolateral flow immunosensor (ELLI); B. ELLI's assay based on modified PEG-stabilized and TEMPO-tagged AuNPs for an amperometric point-of-care detection of dengue NS1 protein. Reprinted with permission from Ref. [132].

4. Wearable Technologies

Wearable and implantable technologies have gained great interest since the introduction of smartphones and mobile devices, due to the possibility of providing a monitoring of the performance and state of health [135–139] and enabling the measurement of clinically relevant parameters in real time [140,141]. The first efforts in this field were mainly addressed through physical sensors for measuring parameters such as mobility, steps, calories burned, or heart rate. With the implementation of new technologies, the demand for wearable devices changed, requiring instrumentation suitable for performing non-invasive analysis on several biomarkers (such as metabolites, hormones, and bacteria) in biofluids, like tears, saliva, urine, sweat, and interstitial fluids. [142] Following this trend, researchers have proposed several examples of wearable biosensors mainly based on electrochemical and optical detection, combined with the most innovative nanomaterials technologies and the use of flexible and advanced materials.

Electrochemical biosensors were the earliest platform that was exploited in the wearable field as they can benefit from easy readout and data processing [143,144]. Lei et al. proposed a stretchable, wearable, and modular multifunctional biosensor, implementing enzymatic assays on MXene/Prussian blue (Ti3C2Tx/PB) electrodes for the detection of glucose, lactate, and pH levels in sweat [145]. The patch-type wearable device consisted of three modules (a sweat-sampling layer, a sensor layer, and a cover layer) and it could be connected to an electrochemical analyzer in order to measure a current signal. Moreover, Wang et al. [146] measured glucose levels in sweat using a gold electrode deposited on the surface of a PET through a procedure that avoided expensive and complex fabrication processes. Zhao et al. [147] reported a fully integrated self-powered smartwatch for the noninvasive and continuous monitoring of glucose levels. The system integrated several components: amorphous silicon (a-Si) photovoltaic cells that can be stored in rechargeable flexible Zn-MnO_2 batteries, providing sufficient power for the operation of the whole system; an electrochemical sensor for measuring glucose in sweat; and a controlling module consisting of a printed circuit board (PCB) and a display to allow direct and real-time monitoring. Lin et al. [148] developed a flexible electrode system based on graphene oxide nanosheets for the impedance measurement of lactate in sweat, exploiting an enzymatic assay involving lactate oxidase. Exploiting the same enzymatic approach for the detection of lactate, Wang et al. [149] also proposed stretchable gold-fiber-based electrodes which were included in textiles in a planar configuration. A different approach was used by Zhang et al. [150] who exploited molecular imprinted polymers (MIP) as a recognition probe. They generated a film of MIP on Ag nanowires which coated the carbon working electrode. MIP allowed us to obtain the selective and sensitive detection of lactate by measuring the differential pulse voltammetry response. Fiore et al. [151] reported on an immunosensor paper-based microfludic device for monitoring cortisol in sweat (Figure 4a). Using wax-printing technology and the laser-cutter technique, they designed a microfluidic pattern that allowed them to perform a competitive immunoassay in which antibodies for the recognition of cortisol were immobilized on magnetic beads and captured on a reaction zone. The competition between cortisol in the sample and cortisol conjugated to a tracer (acetylcholinesterase enzyme) allowed the formation of the analytical signal by folding the pad pre-loaded with the proper enzymatic substrate. By combining this system with a near-field communication wireless module, it was possible to monitor the signal using a smartphone. The same research group also developed a flexible device for monitoring the pH in sweat by depositing an iridium oxide film onto a graphite working electrode, and combining it with an integrated circuit board allows for data acquisition [152].

As well as electrochemical detection, optical detection has also been proposed for its application in wearable biosensors [153–158] (Figure 4b). In this case, some biomarkers have intrinsic optical properties like absorption and emission spectra that allow us to selectively detect these species [159]. Among the applications of the colorimetric approach, several works reported the use of acid–base indicators to measure the pH, allowing for a rapid and reversible detection [160–164]. Generally, these methods are based on naked-eye

evaluation of the color formation which allows us to work with very simple equipment. If a quantitative analysis is required, the use of smartphone cameras as a detector is the most employed solution. A multiplex colorimetric assay for detecting creatinine, pH, and urea was developed by Rogers et al. [165]. The sensor was composed of different areas on which specific reagents for the detection of different target analytes have been immobilized. The colorimetric readout was performed using a smartphone that allowed the quantification, exploiting the RGB analysis system. Optical detection based on the FL principle has been proposed, since the sensitivity offered by FL is higher with respect to colorimetric methods. However, FL implies the requirement of more complex equipment and, therefore, analytical procedure. Xu et al. [166] proposed a wearable Cl^--monitoring platform which combined a flexible cotton piece and two fluorescent materials (lanthanide metal–organic frameworks (MOFs) acting as test and control signals, respectively) by simple ultrasonic loading. The two lanthanide-based fluorescent species allowed for a high color purity and, thus, more precise measurements. Exploiting the smartphone as the detection platform, Cl^- and fluorescence signals were designed for a logic circuit, thus producing a codec device.

The reported examples focus on the non-invasive analysis of sweat or saliva, but these kinds of samples can be insufficient for determining some biomarkers. For this reason, the minimally invasive sampling of intestitial fluid has been proposed, since, compared with other peripheral fluids, it contains much physiological information and shows a strict correlation with blood samples due to the transcapillary exchange between blood and cells [167,168]. Recently, microneedles have gained great success due to the micron size and minimal invasion. [169,170] and they have been widely exploited for sampling interstitial fluid for the detection of several target analytes [171–176], exploiting different principles of extraction (negative pressure, capillary action, swelling force, and ionophoretic). One of the most important applications for microneedle devices is their integration in biosensors for the monitoring of glucose (Table 2). Generally, the electrochemical glucose sensors are based on a reaction that occurs at the working electrode involving glucose [177,178], and it can be classified as enzymatic [179] or non-enzymatic [180,181]. In literature, several devices have been proposed based on the enzymatic reaction between glucose and glucose oxidase and exploiting oxygen as a redox mediator (first generation of glucose-monitoring devices) [182]. In these applications, selectively permeable membranes were used to confined glucose oxidase on the surface of electrodes and to prevent electroactive interference [183–189]. The second generation of glucose sensors employed artificial mediators to avoid oxygen dependence, and is also widely integrated on microneedle-based devices for glucose monitoring [190–198] (Figure 5a). The possibility of exploiting a non-enzymatic reaction allows us to overcome limitations due to the use of the enzyme and to obtain advantages such as good stability, reproducibility, and freedom from oxygen limitation. In this case, generally, the glucose sensors are based on the direct electrochemical oxidation of nanomaterials (i.e., metals, metal-oxides, metal sulfides, metal-organic and metal azolate frameworks, and carbon materials) [199,200]. Several works have been published about the development of microneedle-based monitoring of glucose exploiting these mechanisms [201–203].

The technology of minimally invasive sampling using microneedles for glucose monitoring in interstitial fluid has been extensively proposed also in combination with optical detection. The colorimetric approach is the one that gained much more attention since colorimetric signals can be directly evaluated by the naked eye, or measured by a smartphone camera, and finally elaborated through RGB processing to obtain a quantitative analysis. In this context, the most exploited mechanism is that involving the use of glucose oxidase to generate hydrogen peroxide, which can be used for a subsequent reaction with a chromogenic agent. He et al. [204] proposed a polyvinyl alcohol/chitosan hydrogel integrated with microneedles suitable for the detection of electrolyte ions, glucose, lactate, and proteins, even if the analysis procedure needs a substantial simplification in order to be compatible with the POCT approach. Paper-based platforms have been applied also in combination with these technologies, and several biosensors were reported in literature [205–208]. Besides the production of color on paper located upon microneedles,

different colors can be directly produced on the microneedle patch or even on the skin surface. As an example, Gu et al. [209] developed a transdermal colorimetric microneedle patch comprising two layers: a bottom needle layer functionalized with glucose oxide, and an upper layer in which HRP and TMB were immobilized. The back of the patch became blue as a consequence of the reaction in the presence of glucose and the quantification can be performed by scanning the color intensity with a miniaturized scanner. Yang et al. [210] exploited a microneedle patch made of glucose-oxide-conjugated MnO_2/graphene oxide nanozymes and gelatin methacryloyl. When the interstitial fluid diffused into the patch, the presence of glucose induced the production of H_2O_2, which bound to MnO_2 and promoted the oxidation of TMB on the patch, causing a color change. However, many colorimetric systems rely on the use of enzyme and chromogenic substrates, which can suffer from enzyme denaturation, color quenching, the formation of toxic products, and non-reusability. As an alternative, always exploiting optical detection, FL has been explored for these applications. Zhang et al. [211] proposed an integrated microneedle device with photonic crystal barcodes to enable the multiplex detection of tumor necrosis factor-alpha (TNF-α), interleukin-1β (IL-1β), and IL-6. An FL-conjugated antibody immobilized onto microneedles was used to detect these biomarkers, and the quantification was performed by reading the FL signal of the barcodes (Figure 5b). Moreover, Wang et al. [212] coated the surface of microneedles with antibodies linked to the FL plasmonic fluorophore for the detection of biomarker. Zheng et al. [213] reported on a reagentless biosensor based on an FL-labeled aptamer probe for the on-needle detection of target analytes (glucose, adenosine triphosphate, l-tyrosinamide, and thrombin). By employing strand displacement, the aptamer conjugated to the fluorophore was bound to a DNA competitor strand marked with a quencher species. Sang et al. [214] developed biosensors based on the microneedle array that enabled the emission of an FL signal using a glucose-responsive FL monomer. The monomer has two moieties, one for the recognition of glucose and the other one conjugated to anthracene for FL emission.

Even if the efforts in this field have been increasing, the FL signal is affected by light intensity, probe stability, and variation due to human tissue. Furthermore, the complex procedures and the need for optical instruments limit their diffusion for routinary applications.

Up until now, wearable biosensors based on the use of microneedles available on the market are those for the monitoring of glucose and they are all based on electrochemical detection. Several companies such as Medtronic (Dublin, Ireland), Dexcom (San Diego CA, USA), and Abbott (Chicago, IL, USA) have proposed their devices [215], and they are gaining a great amount of success due to their ease of use, relatively low-cost, and advantages in terms of the real-time monitoring of the health status. Indeed, the short analysis time, as well as the reagentless approach, allows the electrochemical biosensors to be the gold standard for real-time monitoring applications. With the improvements in technologies for optical detection as it concerns the integration with the biosensing element, portability, and the reproducibility of the results, in the future, this detection principle will also be more explored and exploited for the development of biosensors suitable for the market.

Table 2. Comparison of biosensing wearable devices for the quantification of glucose.

Platform	Principle of Detection	Sample	LOD	REF
Skin patch	Electrochemical biosensor incorporating MXene/Prussian blue ($Ti_3C_2T_x$/PB) electrode modified with glucose oxidase.	Sweat	35.3 μA mM^{-1} cm^{-2}	[145]
Sample is collected and then analyzed with the biosensor	Thin-film PET-based gold electrode (PGE) modified with glucose oxidase.	Sweat	2.7 μmol L^{-1}	[146]

Table 2. *Cont.*

Platform	Principle of Detection	Sample	LOD	REF
Flexible sensor integrated into a smartwatch	Enzyme-based sensor integrated into a smartwatch.	Sweat	40 μM	[147]
Skin patch	The metallized microneedle array electrodes were functionalized by entrapping glucose oxidase in electropolymerized polyphenol film.	Dermal interstitial fluid	0.5 mM	[183]
Skin patch	Integration of microneedles into a single biosensor array device containing multiple microcavities for the ectropolymeric entrapment of the glucose oxidase.	Transdermal fluid	0.1 mM	[184]
Transcutaneous implantable sensors	Needle electrodes were coated with polyaniline nanofiber, platinum nanoparticles, and glucose oxidase enzyme.	Transdermal fluid	0.1 mM	[185]
Skin patch	Polylactic-acid-based microneedles were coated with gold as the conductive layer, overoxidized polypyrrol, gold nanoparticles, glucose oxidase, and Nafion.	Interstitial fluid	40 μM	[186]
Skin patch	Microneedle electrode array was fabricated on the flexible substrate using magnetorheological drawing lithography, followed by sputter-coated with Au/Ti film and functionalized with glucose oxidase.	Tested on serum sample	2 mM	[187]
Implantable device to be inserted into the dermis layer	Microneedle array subjected to an electroplating process and to the immobilization of glucose oxidase.	Subcutaneous fluid	1.60 μM	[188]
Skin patch	Microneedle biosensor relies on an ionic liquid (IL)-based carbon paste transducer electrode incorporated with the phenanthroline dione (PD) mediator, followed by a specific enzyme layer, glutaraldehyde (GA) cross-linking, and further coating with chitosan and polyvinyl chloride as outer polymer layers.	Interstitial fluid	1 mM	[187]
Skin patch	Microspike electrochemical array was bonded with a glass slide and modified with glucose oxidase using covalent coupling chemistry.	Interstitial fluid	2 mM	[190]
Skin patch	Integration of modified carbon pastes with glucose oxidase into hollow microneedle devices.	Interstitial fluid	5 mM	[191]
Skin patch	Polymeric microneedle-based working electrodes were doped by enzyme, redox mediator, and photoinitiator.	Interstitial fluid	1 μM	[192]
Skin patch	Bioengineered mussel adhesive protein (MAP) was used for enzyme immobilization on the surface of a microneedle electrode.	Interstitial fluid	100 mg/dL	[193]
Skin patch	Three-electrode system made of Si MNAs whose surface was coated with an thin layer of gold and modified to conjugate dendrimers containing a redox mediator and glucose oxidase.	Interstitial fluid	0.66 mM	[194]

Table 2. *Cont.*

Platform	Principle of Detection	Sample	LOD	REF
Skin patch	Highly porous gold surface of the microneedles was modified by immobilization of a redox mediator and by immobilization of a flavin adenine dinucleotide glucose dehydrogenase (FAD-GDH) enzyme using a drop-casting method.	Interstitial fluid	0.1 mM	[195]
Skin patch	The gold surface of the microneedles was modified by electrodeposition of Au-multiwalled carbon nanotubes and by electropolymerization of the redox mediator and methylene blue (MB), and then modified with glucose oxidase.	Interstitial fluid	3 µM	[196]
Skin patch	FAD-glucose oxidase (GOx) was covalently bound to a terthiophene carboxylic acid (TCA) monomer, followed by electropolymerization on a gold-coated microneedle array.	Tested on blood	0.05 mM	[197]
Skin patch	Non-enzymatic electrochemical sensing based on a multi-walled carbon nanotube forest grown directly on the silicon microneedle array and platinum nano-particles were electrodeposited.	transdermal body fluid	3 mM	[201]
Skin patch	Patch-shaped enzyme-free biosensor using a micro-needle array with Pt-black-sensing electrode layer.	Interstitial fluid	50 µM	[202]
Skin patch	Nafion and platinum black were sequentially coated onto the tip of gold-coated microneedles and used for nonenzymatic (direct) sensing of glucose.	Interstitial fluid	23 µM	[203]

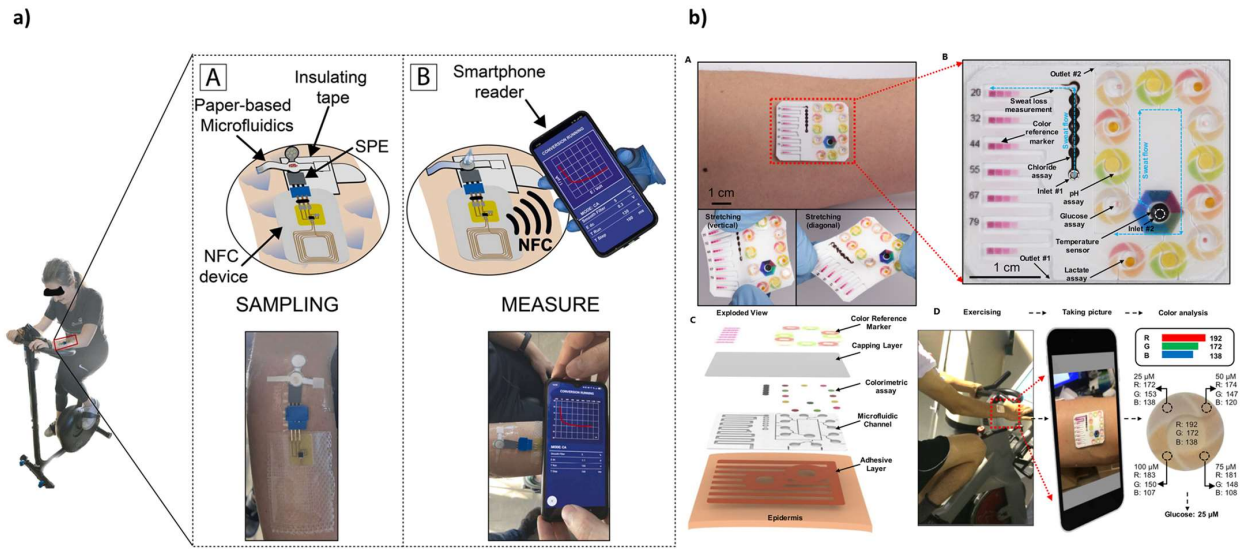

Figure 4. (**a**) Illustration of cortisol during physical activity: A. sampling process; and B. measuring signal and transmitting data to a smartphone via NFC. Reprinted with permission from Ref. [151];

(**b**) Scheme of the microfluidic device for colorimetric analysis of sweat: A. Optical images of microfluidic devices for colorimetric analysis of sweat on the skin (top) and under mechanical deformation with bending (bottom left) and twisting (bottom right); B. Top view of microfluidic channels filled with blue-dyed water; C. Exploded scheme of a device and its interface with the skin; D. Procedure for collecting sweat samples and color analysis of digital images of the device. Reprinted with permission from Ref. [157], Copyright 2019 American Chemical Society.

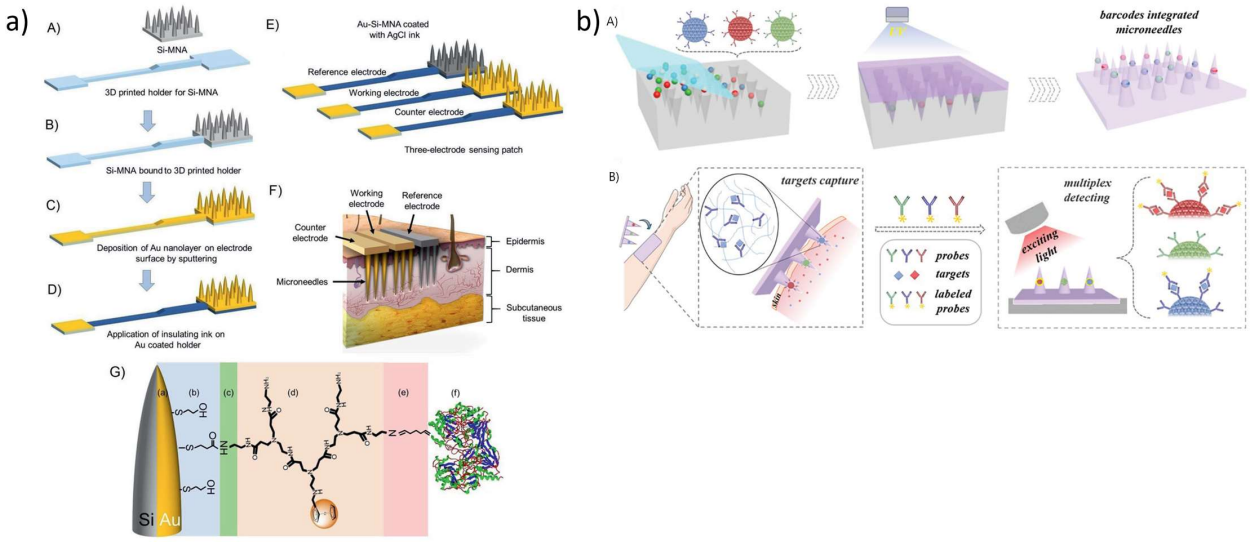

Figure 5. (**a**) Schematic illustration of the high-density silicon MNA electrode preparation: A. Si-MNA and 3D-printed holder; B. Si-MNA substrate attached to the 3D-printed holder; C. Sputter deposition of a thin film of Au; D. insulating ink application; E. Three-electrode sensing patch with Au-Si-MNA as working and counter electrodes, and reference electrode with Au-Si-MNA coated with AgCl ink; F. Schematic of the three-electrode MNA patch penetrating the skin and interfacing with the epidermis and superficial dermis; G. Schematic illustration of the modification of the working electrode. Reproduced with permission from Ref. [194]; (**b**) The generation and application of the encoded MNs: A. Schematic illustration of the fabrication of the encoded MNs by micromolding; B. Schematic illustration of the application of the MNs in ISF detection. Reproduced with permission from Ref. [211].

5. Conclusions and Outlook

In this review are described the advances in the development of POC devices for clinical-medical applications based on optical and electrochemical detection. The most significant efforts have been made in the study of new nanomaterials to by employed, like platforms for bioanalytical assays, innovative strategies for the amplification of analytical signals, and integration within self-standing devices capable of performing the analysis outside centralized laboratories. In many cases, results have been reported that are comparable with those obtained with benchtop instruments that make use of specialized personnel. Despite these enormous steps forward, the most common biosensors in everyday life continue to be the glucometer, with predominantly electrochemical detection, and the pregnancy or COVID-19 tests, mostly based on optical detection. Given the high interest raised from this research field, we will certainly observe an increase in their diffusion and use in the coming years. One of the most significant advances in this sense is represented by wearable devices which have already attracted attention from researchers and which will probably find wide use also for routine applications.

As regards the detection methods, both the electrochemical and optical approaches are equally represented in the literature regarding lab-on-chip and paper-based systems. In the same way, both solutions are widely spread among the commercially available biosensors. The situation changes with wearable biosensors, which, instead, show a strong propensity

for electrochemical detection. Indeed, the application of electrochemical methods seems more immediate and simpler, and its integration with wireless data transmission technology is particularly advantageous. On the contrary, in the context of wearable biosensors, the formation of a signal that must be monitored by an external detector (e.g., CCD, CMOS, and photosensors) does not allow the complete integration of the analytical device and the real-time monitoring of clinical parameters. This will certainly limit the application of optical methods to wearable biosensors, which represent one of the major trends in the field of sensing.

Author Contributions: Conceptualization, M.Z., M.M. and M.G.; writing—original draft preparation, S.R.S.P., A.E., E.L. and A.P.; writing—review and editing, D.C. and M.Z.; supervision, M.Z., M.M. and M.G. All authors have read and agreed to the published version of the manuscript.

Funding: This research was funded by the Italian Ministry of University and Research: PRIN2017 project "Cutting edge analytical chemistry methodologies and bio-tools to boost precision medicine in hormone-related diseases", Prot. 2017Y2PAB8; and PRIN2017 project "Development of novel DNA-based analytical platforms for the rapid, point-of-use quantification of multiple hidden allergens in food samples", Prot. 2017YER72K.

Institutional Review Board Statement: Not applicable.

Informed Consent Statement: Not applicable.

Data Availability Statement: Not applicable.

Conflicts of Interest: The authors declare no conflict of interest.

References

1. *ISO 22870:2016*; Point-of-Care Testing (POCT)—Requirements for Quality and Competence. International Organization for Standardization ISO: Geneva, Switzerland, 2016.
2. Larsson, A.; Greig-Pylypczuk, R.; Huisman, A. The state of point-of-care testing: A European perspective. *Ups J. Med. Sci.* **2015**, *120*, 1–10. [CrossRef] [PubMed]
3. Kozel, T.R.; Burnham-Marusich, A.R. Point-of-Care Testing for Infectious Diseases: Past, Present, and Future. *J. Clin. Microbiol.* **2017**, *55*, 2313. [CrossRef] [PubMed]
4. Vashist, S.K.; Luppa, P.B.; Yeo, L.Y.; Ozcan, A.; Luong, J.H.T. Emerging Technologies for Next-Generation Point-of-Care Testing. *Trends Biotechnol.* **2015**, *33*, 692–705. [CrossRef] [PubMed]
5. Chen, H.; Liu, K.; Li, Z.; Wang, P. Point of care testing for infectious diseases. *Clin. Chim. Acta.* **2019**, *493*, 138–147. [CrossRef] [PubMed]
6. ECDC. *Public Health Guidance on Screening and Vaccination for Infectious Diseases in Newly Arrived Migrants within the EU/EEA*; ECDC: Solna, Sweden, 2018.
7. Reali, S.; Najib, E.Y.; Balázs, K.E.T.; Tan, A.C.H.; Váradi, L.; Hibbs, D.E.; Groundwater, P.W. Novel diagnostics for point-of-care bacterial detection and identification. *RSC Adv.* **2019**, *9*, 21486–21497. [CrossRef] [PubMed]
8. Gopal, A.; Yan, L.; Kashif, S.; Munshi, T.; Roy, V.A.; Voelcker, N.H.; Chen, X. Biosensors and Point-of-Care Devices for Bacterial Detection: Rapid Diagnostics Informing Antibiotic Therapy. *Adv. Health Mat.* **2022**, *11*, 2101546. [CrossRef]
9. Nath, P.; Kabir, A.; Khoubafarin Doust, S.; Kreais, Z.J.; Ray, A. Detection of bacterial and viral pathogens using photonic point-of-care devices. *Diagnostics* **2020**, *10*, 841. [CrossRef]
10. Zhang, Z.; Ma, P.; Ahmed, R.; Wang, J.; Akin, D.; Soto, F.; Demirci, U. Advanced point-of-care testing technologies for human acute respiratory virus detection. *Adv. Mat.* **2022**, *34*, 2103646. [CrossRef]
11. Xiao, M.; Tian, F.; Liu, X.; Zhou, Q.; Pan, J.; Luo, Z.; Yi, C. Virus Detection: From State-of-the-Art Laboratories to Smartphone-Based Point-of-Care Testing. *Adv. Sci.* **2022**, *9*, 2105904. [CrossRef]
12. Zhao, V.X.T.; Wong, T.I.; Zheng, X.T.; Tan, Y.N.; Zhou, X. Colorimetric biosensors for point-of-care virus detections. *Mat. Sci. Energy Technol.* **2020**, *3*, 237–249. [CrossRef]
13. Lu, S.; Lin, S.; Zhang, H.; Liang, L.; Shen, S. Methods of respiratory virus detection: Advances towards point-of-care for early intervention. *Micromachines* **2021**, *12*, 697. [CrossRef] [PubMed]
14. Sohrabi, H.; Bolandi, N.; Hemmati, A.; Eyvazi, S.; Ghasemzadeh, S.; Baradaran, B.; Mokhtarzadeh, A. State-of-the-art cancer biomarker detection by portable (Bio) sensing technology: A critical review. *Microchem. J.* **2022**, *177*, 107248. [CrossRef]
15. Suntornsuk, W.; Suntornsuk, L. Recent applications of paper-based point-of-care devices for biomarker detection. *Electrophoresis* **2020**, *41*, 287–305. [CrossRef] [PubMed]
16. Mahmoudi, T.; de la Guardia, M.; Baradaran, B. Lateral flow assays towards point-of-care cancer detection: A review of current progress and future trends. *TrAC Trends Anal. Chem.* **2020**, *125*, 115842. [CrossRef]

17. Ouyang, M.; Tu, D.; Tong, L.; Sarwar, M.; Bhimaraj, A.; Li, C.; Di Carlo, D. A review of biosensor technologies for blood biomarkers toward monitoring cardiovascular diseases at the point-of-care. *Biosens. Bioelectron.* **2021**, *171*, 112621. [CrossRef]
18. Sachdeva, S.; Davis, R.W.; Saha, A.K. Microfluidic point-of-care testing: Commercial landscape and future directions. *Front. Bioengineer. Biotechnol.* **2021**, *8*, 602659. [CrossRef]
19. Kaur, H.; Bruno, J.G.; Kumar, A.; Sharma, T.K. Aptamers in the therapeutics and diagnostics pipelines. *Theranostics* **2018**, *8*, 4016. [CrossRef]
20. Gui, Q.; Lawson, T.; Shan, S.; Yan, L.; Liu, Y. The application of whole cell-based biosensors for use in environmental analysis and in medical diagnostics. *Sensors* **2017**, *17*, 1623. [CrossRef]
21. Mitchell, K.R.; Esene, J.E.; Woolley, A.T. Advances in multiplex electrical and optical detection of biomarkers using microfluidic devices. *Anal. Bioanal. Chem.* **2022**, *414*, 167–180. [CrossRef]
22. Shi, Y.; Li, Z.; Liu, P.Y.; Nguyen, B.T.T.; Wu, W.; Zhao, Q.; Liu, A.Q. On-Chip Optical Detection of Viruses: A Review. *Adv. Photon Res.* **2021**, *2*, 2000150. [CrossRef]
23. Sezgintürk, M.K. Introduction to commercial biosensors. In *Commercial Biosensors and Their Applications*; Sezgintürk, M.K., Ed.; Elsevier: Amsterdam, The Netherlands, 2020; pp. 1–28.
24. Haleem, A.; Javaid, M.; Singh, R.P.; Suman, R.; Rab, S. Biosensors applications in medical field: A brief review. *Sens. Int.* **2021**, *2*, 100100. [CrossRef]
25. Anfossi, L.; Di Nardo, F.; Russo, A.; Cavalera, S.; Giovannoli, C.; Spano, G.; Baggiani, C. Silver and gold nanoparticles as multi-chromatic lateral flow assay probes for the detection of food allergens. *Anal. Bioanal. Chem.* **2019**, *411*, 1905–1913. [CrossRef] [PubMed]
26. Di Nardo, F.; Baggiani, C.; Giovannoli, C.; Spano, G.; Anfossi, L. Multicolor immunochromatographic strip test based on gold nanoparticles for the determination of aflatoxin B1 and fumonisins. *Microchim. Acta* **2017**, *184*, 1295–1304. [CrossRef]
27. Quang, L.X.; Lim, C.; Seong, G.H.; Choo, J.; Do, K.J.; Yoo, S.K. A portable surface-enhanced Raman scattering sensor integrated with a lab-on-a-chip for field analysis. *Lab Chip* **2008**, *8*, 2214–2219. [CrossRef] [PubMed]
28. Xu, K.; Zhou, R.; Takei, K.; Hong, M. Toward flexible surface-enhanced Raman scattering (SERS) sensors for point-of-care diagnostics. *Adv. Sci.* **2019**, *6*, 1900925. [CrossRef]
29. Hamm, L.; Gee, A.; De Silva Indrasekara, A.S. Recent advancement in the surface-enhanced Raman spectroscopy-based biosensors for infectious disease diagnosis. *Appl. Sci.* **2019**, *9*, 1448. [CrossRef]
30. Choi, N.; Lee, J.; Ko, J.; Jeon, J.H.; Rhie, G.E.; deMello, A.J.; Choo, J. Integrated SERS-based microdroplet platform for the automated immunoassay of F1 antigens in Yersinia pestis. *Anal. Chem.* **2017**, *89*, 8413–8420. [CrossRef]
31. Roda, A.; Mirasoli, M.; Michelini, E.; Di Fusco, M.; Zangheri, M.; Cevenini, L.; Simoni, P. Progress in chemical luminescence-based biosensors: A critical review. *Biosens. Bioelectron.* **2016**, *76*, 164–179. [CrossRef]
32. Calabretta, M.M.; Lopreside, A.; Montali, L.; Zangheri, M.; Evangelisti, L.; D'Elia, M.; Michelini, E. Portable light detectors for bioluminescence biosensing applications: A comprehensive review from the analytical chemist's perspective. *Anal. Chim. Acta* **2022**, *1200*, 339583. [CrossRef]
33. Mirasoli, M.; Nascetti, A.; Caputo, D.; Zangheri, M.; Scipinotti, R.; Cevenini, L.; de Cesare, G.; Roda, A. Multiwell cartridge with integrated array of amorphous silicon photosensors for chemiluminescence detection: Development, characterization and comparison with cooled-CCD luminograph. *Anal Bioanal Chem.* **2014**, *406*, 5645–5656. [CrossRef]
34. Zangheri, M.; Mirasoli, M.; Nascetti, A.; Caputo, D.; Bonvicini, F.; Gallinella, G.; Roda, A. Microfluidic cartridge with integrated array of amorphous silicon photosensors for chemiluminescence detection of viral DNA. *Sens. Biosens. Res.* **2016**, *7*, 127–132. [CrossRef]
35. Caputo, D.; de Cesare, G.; Scipinotti, R.; Mirasoli, M.; Roda, A.; Zangheri, M.; Nascetti, A. Chemiluminescence-Based Micro-total-Analysis System with Amorphous Silicon Photodiodes. In *Sensors and Microsystems*; Springer International Publishing: Cham, Switzerland, 2014; pp. 207–211.
36. Lazzarini, E.; Pace, A.; Trozzi, I.; Zangheri, M.; Guardigli, M.; Calabria, D.; Mirasoli, M. An Origami Paper-Based Biosensor for Allergen Detection by Chemiluminescence Immunoassay on Magnetic Microbeads. *Biosensors* **2022**, *12*, 825. [CrossRef] [PubMed]
37. Sciutto, G.; Zangheri, M.; Anfossi, L.; Guardigli, M.; Prati, S.; Mirasoli, M.; Roda, A. Miniaturized biosensors to preserve and monitor cultural heritage: From medical to conservation diagnosis. *Angew. Chem.* **2018**, *130*, 7507–7511. [CrossRef]
38. Zangheri, M.; Di Nardo, F.; Calabria, D.; Marchegiani, E.; Anfossi, L.; Guardigli, M.; Roda, A. Smartphone biosensor for point-of-need chemiluminescence detection of ochratoxin A in wine and coffee. *Anal. Chim. Acta* **2021**, *1163*, 338515. [CrossRef]
39. Roda, A.; Calabretta, M.M.; Calabria, D.; Caliceti, C.; Cevenini, L.; Lopreside, A.; Zangheri, M. Smartphone-based biosensors. Past, Present and Future Challenges of Biosensors and Bioanalytical Tools in Analytical Chemistry: A Tribute to Professor Marco Mascini. *Compr. Anal. Chem.* **2017**, *77*, 237–286.
40. Calabria, D.; Zangheri, M.; Trozzi, I.; Lazzarini, E.; Pace, A.; Mirasoli, M.; Guardigli, M. Smartphone-based chemiluminescent origami μPAD for the rapid assessment of glucose blood levels. *Biosensors* **2021**, *11*, 381. [CrossRef]
41. Di Fusco, M.; Quintavalla, A.; Lombardo, M.; Guardigli, M.; Mirasoli, M.; Trombini, C.; Roda, A. Organically modified silica nanoparticles doped with new acridine-1, 2-dioxetane analogues as thermochemiluminescence reagentless labels for ultrasensitive immunoassays. *Anal. Bioanal. Chem.* **2015**, *407*, 1567–1576. [CrossRef]
42. Roda, A.; Michelini, E.; Zangheri, M.; Di Fusco, M.; Calabria, D.; Simoni, P. Smartphone-based biosensors: A critical review and perspectives. *TrAC Trends Anal. Chem.* **2016**, *79*, 317–325. [CrossRef]

43. Bahadır, E.B.; Sezgintürk, M.K. Electrochemical biosensors for hormone analyses. *Biosens. Bioelectron.* **2015**, *68*, 62–71. [CrossRef]
44. Chakraborty, A.; Tibarewala, D.N.; Barui, A. Impedance-based biosensors. *Bioelectron. Med. Devices* **2019**, 97–122. [CrossRef]
45. Richter, M.M. Electrochemiluminescence (ecl). *Chem. Rev.* **2004**, *104*, 3003–3036. [CrossRef] [PubMed]
46. Miao, W. Electrogenerated chemiluminescence and its biorelated applications. *Chem. Rev.* **2008**, *108*, 2506–2553. [CrossRef]
47. Du, F.; Chen, Y.; Meng, C.; Lou, B.; Zhang, W.; Xu, G. Recent advances in electrochemiluminescence immunoassay based on multiple-signal strategy. *Current Opin. Electrochem.* **2021**, *28*, 100725. [CrossRef]
48. Nasrollahpour, H.; Khalilzadeh, B.; Naseri, A.; Sillanpaa, M.; Chia, C.H. Homogeneous electrochemiluminescence in the sensors game: What have we learned from past experiments? *Anal. Chem.* **2021**, *94*, 349–365. [CrossRef] [PubMed]
49. Ma, X.; Gao, W.; Du, F.; Yuan, F.; Yu, J.; Guan, Y.; Xu, G. Rational design of electrochemiluminescent devices. *Acc. Chem. Res.* **2021**, *54*, 2936–2945. [CrossRef]
50. Nikolaou, P.; Sciuto, E.L.; Zanut, A.; Petralia, S.; Valenti, G.; Paolucci, F.; Conoci, S. Ultrasensitive PCR-Free detection of whole virus genome by electrochemiluminescence. *Biosens. Bioelectron.* **2022**, *209*, 114165. [CrossRef]
51. Yoo, S.M.; Jeon, Y.M.; Heo, S.Y. Electrochemiluminescence Systems for the Detection of Biomarkers: Strategical and Technological Advances. *Biosensors* **2022**, *12*, 738. [CrossRef]
52. Kholafazad-Kordasht, H.; Hasanzadeh, M.; Seidi, F. Smartphone based immunosensors as next generation of healthcare tools: Technical and analytical overview towards improvement of personalized medicine. *Trends Anal. Chem.* **2021**, *145*, 116455. [CrossRef]
53. Sun, A.C.; Hall, D.A. Point-of-care smartphone-based electrochemical biosensing. *Electroanalysis* **2019**, *31*, 2–16. [CrossRef]
54. Nascetti, A.; Mirasoli, M.; Marchegiani, E.; Zangheri, M.; Costantini, F.; Porchetta, A.; Roda, A. Integrated chemiluminescence-based lab-on-chip for detection of life markers in extraterrestrial environments. *Biosens. Bioelectron.* **2019**, *123*, 195–203. [CrossRef]
55. Zhang, T.; Chakrabarty, K.; Fair, R.B. *Microelectrofluidic Systems: Modeling and Simulation*; CRC Press: Boca Raton, FL, USA, 2018.
56. Reyes, D.R.; Iossifidis, D.; Auroux, P.A.; Manz, P.A. Micro total analysis systems: 1. Introduction, theory, and technology. *Anal. Chem.* **2002**, *74*, 2623–2636. [CrossRef] [PubMed]
57. Auroux, A.; Reyes, D.R.; Iossifidis, D.; Manz, P.A. Micro total analysis systems: 2. Analytical standard operations and applications. *Anal. Chem.* **2002**, *74*, 2637–2652. [CrossRef] [PubMed]
58. West, J.; Becker, M.; Tombrink, S.; Manz, A. Micro total analysis systems: Latest achievements. *Anal. Chem.* **2008**, *80*, 4403–4419. [CrossRef]
59. Giannitsis, A.T. Microfabrication of biomedical lab-on-chip devices. A review. *Estonian J. Eng.* **2011**, *17*, 109. [CrossRef]
60. Zhang, W.; Wang, R.; Luo, F.; Wang, P.; Lin, Z. Miniaturized electrochemical sensors and their point-of-care applications. *Chin. Chem. Let.* **2020**, *31*, 589–600. [CrossRef]
61. Ainla, A.; Mousavi, M.P.; Tsaloglou, M.N.; Redston, J.; Bell, J.G.; Fernández-Abedul, M.T.; Whitesides, G.M. Open-source potentiostat for wireless electrochemical detection with smartphones. *Anal Chem.* **2018**, *90*, 6240–6246. [CrossRef]
62. Dryden, M.D.; Wheeler, A.R. DStat: A versatile, open-source potentiostat for electroanalysis and integration. *PLoS ONE* **2015**, *10*, e0140349. [CrossRef]
63. Rowe, A.A.; Bonham, A.J.; White, R.J.; Zimmer, M.P.; Yadgar, R.J.; Hobza, T.M.; Plaxco, K.W. CheapStat: An open-source, "Do-It-Yourself" potentiostat for analytical and educational applications. *PLoS ONE* **2011**, *6*, e23783. [CrossRef]
64. Dobbelaere, T.; Vereecken, P.M.; Detavernier, C. A USB-controlled potentiostat/galvanostat for thin-film battery characterization. *HardwareX* **2017**, *2*, 34–49. [CrossRef]
65. Lopin, P.; Lopin, K.V. PSoC-Stat: A single chip open source potentiostat based on a Programmable System on a Chip. *PLoS ONE* **2018**, *13*, e0201353. [CrossRef]
66. Beach, R.D.; Conlan, R.W.; Godwin, M.C.; Moussy, F. Towards a miniature implantable in vivo telemetry monitoring system dynamically configurable as a potentiostat or galvanostat for two-and three-electrode biosensors. *IEEE Trans. Instrum. Meas.* **2005**, *54*, 61–72. [CrossRef]
67. Ferrari, A.G.M.; Rowley-Neale, S.J.; Banks, C.E. Screen-printed electrodes: Transitioning the laboratory in-to-the field. *Talanta Open* **2021**, *3*, 100032. [CrossRef]
68. Ferrari, A.G.M.; Amor-Gutiérrez, O.; Costa-Rama, E.; Fernández-Abedul, M.T. Batch injection electroanalysis with stainless-steel pins as electrodes in single and multiplexed configurations. *Sens. Actuat B Chem.* **2017**, *253*, 1207–1213. [CrossRef]
69. Foster, C.W.; Kadara, R.O.; Banks, C.E. *Screen-Printing Electrochemical Architectures*; Springer: Berlin, Germany, 2016.
70. Giacomelli, C.E.; Vermeer, A.W.P.; Norde, W. Adsorption of immunoglobulin G on core-shell latex particles precoated with chaps. *J. Colloid Interf. Sci.* **2000**, *231*, 283–288. [CrossRef] [PubMed]
71. Charelier, R.C.; Gengenbach, T.R.; Griesser, H.J.; Brigham-Burke, M.; O'Shannessy, D.J. A general method to recondition and reuse BIAcore sensor chips fouled with covalently immobilized protein/peptide. *Anal. Biochem.* **1995**, *229*, 112–118. [CrossRef]
72. Charles, P.T.; Goldman, E.R.; Rangasammy, J.G.; Schauer, C.L.; Chen, M.S.; Taitt, C.R. Fabrication and characterization of 3D hydrogel microarrays to measure antigenicity and antibody functionality for biosensor application. *Biosens. Bioelectron.* **2004**, *20*, 753–764. [CrossRef]
73. Palma, R.; Borghs, G.; Declerck, P.; Goddeeris, B. Comparison of random and oriented immobilization of antibody fragments on mixed self-assembled monolayers. *J. Immunol. Methods* **2006**, *312*, 167–181.
74. Hu, T.; Zhang, M.; Wang, Z.; Chen, K.; Li, X.; Ni, Z. Layer-by-layer self-assembly of MoS_2/PDDA hybrid film in microfluidic chips for ultrasensitive electrochemical immunosensing of alpha-fetoprotein. *Microchem. J.* **2020**, *158*, 105209. [CrossRef]

75. Timilsina, S.S.; Ramasamy, M.; Durr, N.; Ahmad, R.; Jolly, P.; Ingber, D.E. Biofabrication of Multiplexed Electrochemical Immunosensors for Simultaneous Detection of Clinical Biomarkers in Complex Fluids. *Adv. Health Mat.* **2022**, *11*, 2200589. [CrossRef]
76. Escamilla-Gómez, V.; Hernández-Santos, D.; González-García, M.B.; Pingarrón-Carrazón, J.M.; Costa-García, A. Simultaneous detection of free and total prostate specific antigen on a screen-printed electrochemical dual sensor. *Biosens. Bioelectron.* **2009**, *24*, 2678–2683. [CrossRef]
77. Singh, R.; Hong, S.; Jang, J. Label-free detection of influenza viruses using a reduced Graphene oxide-based electrochemical immunosensor integrated with a microfluidic platform. *Sci. Rep.* **2017**, *7*, 4277. [CrossRef]
78. Roberts, A.; Chauhan, N.; Islam, S.; Mahari, S.; Ghawri, B.; Gandham, R.K.; Gandhi, S. Graphene functionalized field-effect transistors for ultrasensitive detection of Japanese encephalitis and Avian influenza virus. *Sci. Rep.* **2020**, *10*, 14546. [CrossRef] [PubMed]
79. Ono, T.; Oe, T.; Kanai, Y.; Ikuta, T.; Ohno, Y.; Maehashi, K.; Matsumoto, K. Glycan-functionalized graphene-FETs toward selective detection of human-infectious avian influenza virus. *Jpn. J. Appl. Phys.* **2017**, *56*, 030302. [CrossRef]
80. Maity, A.; Sui, X.; Jin, B.; Pu, H.; Bottum, K.J.; Huang, X.; Chen, J. Resonance-frequency modulation for rapid, point-of-care Ebola-Glycoprotein diagnosis with a graphene-based field-effect biotransistor. *Anal Chem.* **2018**, *90*, 14230–14238. [CrossRef] [PubMed]
81. Jin, X.; Zhang, H.; Li, Y.T.; Xiao, M.M.; Zhang, Z.L.; Pang, D.W.; Zhang, G.J. A field effect transistor modified with reduced graphene oxide for immunodetection of Ebola virus. *Microchim. Acta.* **2019**, *186*, 223. [CrossRef]
82. Sengupta, J.; Adhikari, A.; Hussain, C.M. Graphene-based analytical lab-on-chip devices for detection of viruses: A review. *Carbon Trends* **2021**, *4*, 100072. [CrossRef]
83. Seo, G.; Lee, G.; Kim, M.J.; Baek, S.H.; Choi, M.; Ku, K.B.; Kim, S.I. Rapid detection of COVID-19 causative virus (SARS-CoV-2) in human nasopharyngeal swab specimens using field-effect transistor-based biosensor. *ACS Nano* **2020**, *14*, 5135–5142. [CrossRef]
84. Zhao, H.; Liu, F.; Xie, W.; Zhou, T.C.; OuYang, J.; Jin, L.; Li, C.P. Ultrasensitive supersandwich-type electrochemical sensor for SARS-CoV-2 from the infected COVID-19 patients using a smartphone. *Sens. Actuat B Chem.* **2021**, *327*, 128899. [CrossRef]
85. Ali, M.A.; Hu, C.; Jahan, S.; Yuan, B.; Saleh, M.S.; Ju, E.; Panat, R. Sensing of COVID-19 antibodies in seconds via aerosol jet nanoprinted reduced-graphene-oxide-coated 3D electrodes. *Adv. Mat.* **2021**, *33*, 2006647. [CrossRef]
86. Roda, A.; Arduini, F.; Mirasoli, M.; Zangheri, M.; Fabiani, L.; Colozza, N.; Moscone, D. A challenge in biosensors: Is it better to measure a photon or an electron for ultrasensitive detection? *Biosens. Bioelectron.* **2020**, *155*, 112093. [CrossRef]
87. Iinuma, M.; Kadoya, Y.; Kuroda, A. Photon counting system for high-sensitivity detection of bioluminescence at optical fiber end. *Biolumin. Methods Protoc.* **2016**, *1461*, 299–310.
88. Calabria, D.; Trozzi, I.; Lazzarini, E.; Pace, A.; Zangheri, M.; Iannascoli, L.; Mirasoli, M. AstroBio-CubeSat: A lab-in-space for chemiluminescence-based astrobiology experiments. *Biosens. Bioelectron.* **2023**, *226*, 115110. [CrossRef] [PubMed]
89. Dinter, F.; Burdukiewicz, M.; Schierack, P.; Lehmann, W.; Nestler, J.; Dame, G.; Rödiger, S. Simultaneous detection and quantification of DNA and protein biomarkers in spectrum of cardiovascular diseases in a microfluidic microbead chip. *Anal Bioanal. Chem.* **2019**, *411*, 7725–7735. [CrossRef] [PubMed]
90. Chang, N.; Zhai, J.; Liu, B.; Zhou, J.; Zeng, Z.; Zhao, X. Low cost 3D microfluidic chips for multiplex protein detection based on photonic crystal beads. *Lab Chip* **2018**, *18*, 3638–3644. [CrossRef] [PubMed]
91. Yuan, X.; Garg, S.; De Haan, K.; Fellouse, F.A.; Gopalsamy, A.; Tykvart, J.; Aitchison, J.S. Bead-based multiplex detection of dengue biomarkers in a portable imaging device. *Biomed. Opt. Express* **2020**, *11*, 6154–6167. [CrossRef] [PubMed]
92. Dai, B.; Yin, C.; Wu, J.; Li, W.; Zheng, L.; Lin, F.; Zhuang, S. A flux-adaptable pump-free microfluidics-based self-contained platform for multiplex cancer biomarker detection. *Lab Chip* **2021**, *21*, 143–153. [CrossRef]
93. Sharafeldin, M.; Chen, T.; Ozkaya, G.U.; Choudhary, D.; Molinolo, A.A.; Gutkind, J.S.; Rusling, J.F. Detecting cancer metastasis and accompanying protein biomarkers at single cell levels using a 3D-printed microfluidic immunoarray. *Biosens. Bioelectron.* **2021**, *171*, 112681. [CrossRef]
94. Mirasoli, M.; Bonvicini, F.; Lovecchio, N.; Petrucci, G.; Zangheri, M.; Calabria, D.; Nascetti, A. On-chip LAMP-BART reaction for viral DNA real-time bioluminescence detection. *Sensors Actuat. B Chem.* **2018**, *262*, 1024–1033. [CrossRef]
95. Calabria, D.; Lazzarini, E.; Pace, A.; Trozzi, I.; Zangheri, M.; Cinti, S.; Mirasoli, M. Smartphone-based 3D-printed electrochemiluminescence enzyme biosensor for reagentless glucose quantification in real matrices. *Biosens. Bioelectron.* **2023**, *227*, 115146. [CrossRef] [PubMed]
96. Carrell, C.; Kava, A.; Nguyen, M.; Menger, R.; Munshi, Z.; Call, Z.; Henry, C. Beyond the lateral flow assay: A review of paper-based microfluidics. *Microelectron. Eng.* **2019**, *206*, 45–54. [CrossRef]
97. He, Y.; Wu, Y.; Fu, J.Z.; Wu, W.B. Fabrication of paper-based microfluidic analysis devices: A review. *RSC Adv.* **2015**, *5*, 78109–78127. [CrossRef]
98. Lee, V.B.C.; Mohd-Naim, N.F.; Tamiya, E.; Ahmed, M.U. Trends in paper-based electrochemical biosensors: From design to application. *Anal. Sci.* **2018**, *34*, 7–18. [CrossRef] [PubMed]
99. Tran, V.K.; Ko, E.; Geng, Y.; Kim, M.K.; Jin, G.H.; Son, S.E.; Seong, G.H. Micro-patterning of single-walled carbon nanotubes and its surface modification with gold nanoparticles for electrochemical paper-based non-enzymatic glucose sensor. *J. Electroanal. Chem.* **2018**, *826*, 29–37. [CrossRef]

100. Punjiya, M.; Moon, C.H.; Matharu, Z.; Nejad, H.R.; Sonkusale, S. A three-dimensional electrochemical paper-based analytical device for low-cost diagnostics. *Analyst* **2018**, *143*, 1059–1064. [CrossRef]
101. Amor-Gutiérrez, O.; Costa-Rama, E.; Fernández-Abedul, M.T. Sampling and multiplexing in lab-on-paper bioelectroanalytical devices for glucose determination. *Biosens. Bioelectron.* **2019**, *135*, 64–70. [CrossRef]
102. He, X.; Chang, S.J.; Settu, K.; Chen, C.J.; Liu, J.T. An anti-HCT-interference glucose sensor based on a fiber paper-based screen-printed carbon electrode. *Sensors Actua B Chem.* **2019**, *297*, 126763. [CrossRef]
103. Mohammadifar, M.; Tahernia, M.; Choi, S. An equipment-free, paper-based electrochemical sensor for visual monitoring of glucose levels in urine. *SLAS Technol. Transl. Life Sci. Inn.* **2019**, *24*, 499–505. [CrossRef]
104. Calabria, D.; Pace, A.; Lazzarini, E.; Trozzi, I.; Zangheri, M.; Guardigli, M.; Mirasoli, M. Smartphone-Based Chemiluminescence Glucose Biosensor Employing a Peroxidase-Mimicking, Guanosine-Based Self-Assembled Hydrogel. *Biosensors* **2023**, *13*, 650. [CrossRef] [PubMed]
105. Cao, Q.; Liang, B.; Yu, C.; Fang, L.; Tu, T.; Wei, J.; Ye, X. High accuracy determination of multi metabolite by an origami-based coulometric electrochemical biosensor. *J. Electroanal. Chem.* **2020**, *873*, 114358. [CrossRef]
106. Rafatmah, E.; Hemmateenejad, B. Dendrite gold nanostructures electrodeposited on paper fibers: Application to electrochemical non-enzymatic determination of glucose. *Sens. Actuat. B Chem.* **2020**, *304*, 127335. [CrossRef]
107. Pesaran, S.; Rafatmah, E.; Hemmateenejad, B. An all-in-one solid state thin-layer potentiometric sensor and biosensor based on three-dimensional origami paper microfluidics. *Biosensors* **2021**, *11*, 44. [CrossRef] [PubMed]
108. Urusov, A.E.; Zherdev, A.V.; Dzantiev, B.B. Towards lateral flow quantitative assays: Detection approaches. *Biosensors* **2019**, *9*, 89. [CrossRef] [PubMed]
109. Urusov, A.E.; Jerdev, A.V.; Starovoitova, T.A.; Vengerov, Y.Y.; Dzantiev, B.B. The device registration of immune chromatographic express-tests. *Klin. Lab. Diagn.* **2016**, *61*, 173–179. [PubMed]
110. Zangheri, M.; Mirasoli, M.; Guardigli, M.; Di Nardo, F.; Anfossi, L.; Baggiani, C.; Roda, A. Chemiluminescence-based biosensor for monitoring astronauts' health status during space missions: Results from the International Space Station. *Biosens. Bioelectron.* **2019**, *129*, 260–268. [CrossRef]
111. Yang, J.; Wang, K.; Xu, H.; Yan, W.; Jin, Q.; Cui, D. Detection platforms for point-of-care testing based on colorimetric, luminescent and magnetic assays: A review. *Talanta* **2019**, *202*, 96–110. [CrossRef]
112. Park, J. Lateral Flow Immunoassay Reader Technologies for Quantitative Point-of-Care Testing. *Sensors* **2022**, *22*, 7398. [CrossRef]
113. Firdaus, M.L.; Alwi, W.; Trinoveldi, F.; Rahayu, I.; Rahmidar, L.; Warsito, K. Determination of Chromium and Iron Using Digital Image-based Colorimetry. *Procedia Environ. Sci.* **2014**, *20*, 298–304. [CrossRef]
114. Lee, A.S.; Kim, S.M.; Kim, K.R.; Park, C.; Lee, D.G.; Heo, H.R.; Kim, C.S. A colorimetric lateral flow immunoassay based on oriented antibody immobilization for sensitive detection of SARS-CoV-2. *Sens. Actuat. B Chem.* **2023**, *379*, 133245. [CrossRef]
115. Han, H.; Wang, C.; Yang, X.; Zheng, S.; Cheng, X.; Liu, Z.; Xiao, R. Rapid field determination of SARS-CoV-2 by a colorimetric and fluorescent dual-functional lateral flow immunoassay biosensor. *Sens. Actuat. B Chem.* **2022**, *351*, 130897. [CrossRef]
116. Roda, A.; Cavalera, S.; Di Nardo, F.; Calabria, D.; Rosati, S.; Simoni, P.; Anfossi, L. Dual lateral flow optical/chemiluminescence immunosensors for the rapid detection of salivary and serum IgA in patients with COVID-19 disease. *Biosens. Bioelectron.* **2021**, *172*, 112765. [CrossRef]
117. Li, H.; Ying, Y.; Cao, Z.; Liu, G.; Wang, J. Research progress on rapid detection technology based on smartphone and lateral flow immunoassay. *Chin. J. Anal. Chem.* **2022**, *50*, 1–11.
118. Pohanka, M. Point-of-care diagnoses and assays based on lateral flow test. *Int. J. Anal. Chem.* **2021**, *2021*, 6685619. [CrossRef]
119. Calabria, D.; Calabretta, M.M.; Zangheri, M.; Marchegiani, E.; Trozzi, I.; Guardigli, M.; Mirasoli, M. Recent advancements in enzyme-based lateral flow immunoassays. *Sensors* **2021**, *21*, 3358. [CrossRef] [PubMed]
120. Li, J.; Liu, B.; Tang, X.; Wu, Z.; Lu, J.; Liang, C.; Li, C. Development of a smartphone-based quantum dot lateral flow immunoassay strip for ultrasensitive detection of anti-SARS-CoV-2 IgG and neutralizing antibodies. *Int. J. Infect Dis.* **2022**, *121*, 58–65. [CrossRef]
121. Mahmoud, M.; Ruppert, C.; Rentschler, S.; Laufer, S.; Deigner, H.P. Combining aptamers and antibodies: Lateral flow quantification for thrombin and interleukin-6 with smartphone readout. *Sens. Actuat. B Chem.* **2021**, *333*, 129246. [CrossRef]
122. Rong, Z.; Wang, Q.; Sun, N.; Jia, X.; Wang, K.; Xiao, R.; Wang, S. Smartphone-based fluorescent lateral flow immunoassay platform for highly sensitive point-of-care detection of Zika virus nonstructural protein 1. *Anal. Chim. Acta* **2019**, *1055*, 140–147. [CrossRef]
123. Chabi, M.; Vu, B.; Brosamer, K.; Smith, M.; Chavan, D.; Conrad, J.C.; Kourentzi, K. Smartphone-read phage lateral flow assay for point-of-care detection of infection. *Analyst* **2023**, *148*, 839–848. [CrossRef]
124. Ren, Z.; Xu, L.; Yang, L.; Cui, Y. Minimizing Cross-Reactivity for the Chemiluminescent Lateral Flow Immunoassay of Cardiac Troponin I Based on PEGylation of Gold Nanoparticles. *Anal. Chem.* **2023**, *95*, 6646–6654. [CrossRef]
125. Roda, A.; Zangheri, M.; Calabria, D.; Mirasoli, M.; Caliceti, C.; Quintavalla, A.; Simoni, P. A simple smartphone-based thermo-chemiluminescent immunosensor for valproic acid detection using 1, 2-dioxetane analogue-doped nanoparticles as a label. *Sens. Actuat. B Chem.* **2019**, *279*, 327–333. [CrossRef]
126. Mazurkiewicz, W.; Podrażka, M.; Jarosińska, E.; Kappalakandy Valapil, K.; Wiloch, M.; Jönsson-Niedziółka, M.; Witkowska Nery, E. Paper-Based Electrochemical Sensors and How to Make Them (Work). *ChemElectroChem* **2020**, *7*, 2939–2956. [CrossRef]
127. Arduini, F. Electrochemical paper-based devices: When the simple replacement of the support to print ecodesigned electrodes radically improves the features of the electrochemical devices. *Curr. Opin. Electrochem.* **2022**, *35*, 101090. [CrossRef]

128. Dungchai, W.; Chailapakul, O.; Henry, C.S. Electrochemical detection for paper-based microfluidics. *Anal. Chem.* **2009**, *81*, 5821–5826. [CrossRef] [PubMed]
129. Noviana, E.; McCord, C.P.; Clark, K.M.; Jang, I.; Henry, C.S. Electrochemical paper-based devices: Sensing approaches and progress toward practical applications. *Lab Chip.* **2020**, *20*, 9–34. [CrossRef] [PubMed]
130. Cheng, J.; Yang, G.; Guo, J.; Liu, S.; Guo, J. Integrated electrochemical lateral flow immunoassays (eLFIAs): Recent advances. *Analyst* **2022**, *147*, 554–570. [CrossRef] [PubMed]
131. Deenin, W.; Yakoh, A.; Pimpitak, U.; Pasomsub, E.; Rengpipat, S.; Crespo, G.A.; Chaiyo, S. Electrochemical lateral-flow device for rapid COVID-19 antigen-diagnostic testing. *Bioelectrochem* **2023**, *152*, 108438. [CrossRef] [PubMed]
132. Sinawang, P.D.; Fajs, L.; Elouarzaki, K.; Nugraha, J.; Marks, R.S. TEMPO-based immuno-lateral flow quantitative detection of dengue NS1 protein. *Sens. Actuat. B Chem.* **2018**, *259*, 354–363. [CrossRef]
133. Srisomwat, C.; Yakoh, A.; Chuaypen, N.; Tangkijvanich, P.; Vilaivan, T.; Chailapakul, O. Amplification-free DNA sensor for the one-step detection of the hepatitis B virus using an automated paper-based lateral flow electrochemical device. *Anal. Chem.* **2020**, *93*, 2879–2887. [CrossRef]
134. Hong, D.; Jo, E.J.; Kim, K.; Song, M.B.; Kim, M.G. Ru $(bpy)_3^{2+}$-loaded mesoporous silica nanoparticles as electrochemiluminescent probes of a lateral flow immunosensor for highly sensitive and quantitative detection of troponin I. *Small* **2020**, *16*, 2004535. [CrossRef]
135. Bandodkar, A.J.; Jeerapan, I.; Wang, J. Wearable chemical sensors: Present challenges and future prospects. *ACS Sens.* **2016**, *1*, 464–482. [CrossRef]
136. Heikenfeld, J.; Jajack, A.; Rogers, J.; Gutruf, P.; Tian, L.; Pan, T.; Wang, J. Wearable sensors: Modalities, challenges, and prospects. *Lab Chip.* **2018**, *18*, 217–248. [CrossRef]
137. Liu, Y.; Pharr, M.; Salvatore, G.A. Lab-on-skin: A review of flexible and stretchable electronics for wearable health monitoring. *ACS Nano* **2017**, *11*, 9614–9635. [CrossRef] [PubMed]
138. Amjadi, M.; Kyung, K.U.; Park, I.; Sitti, M. Stretchable, skin-mountable, and wearable strain sensors and their potential applications: A review. *Adv. Funct. Mater.* **2016**, *26*, 1678–1698. [CrossRef]
139. Bariya, M.; Nyein, H.Y.Y.; Javey, A. Wearable sweat sensors. *Nat. Electron.* **2018**, *1*, 160–171. [CrossRef]
140. Roda, A.; Mirasoli, M.; Guardigli, M.; Zangheri, M.; Caliceti, C.; Calabria, D.; Simoni, P. Advanced biosensors for monitoring astronauts' health during long-duration space missions. *Biosens. Bioelectron.* **2018**, *111*, 18–26. [CrossRef]
141. Calabretta, M.M.; Zangheri, M.; Lopreside, A.; Marchegiani, E.; Montali, L.; Simoni, P.; Roda, A. Precision medicine, bioanalytics and nanomaterials: Toward a new generation of personalized portable diagnostics. *Analyst* **2020**, *145*, 2841–2853. [CrossRef]
142. Kim, J.; Campbell, A.S.; de Ávila, B.E.F.; Wang, J. Wearable biosensors for healthcare monitoring. *Nat. Biotechnol.* **2019**, *37*, 389–406. [CrossRef]
143. Grieshaber, D.; MacKenzie, R.; Vörös, J.; Reimhult, E. Electrochemical biosensors-sensor principles and architectures. *Sensors* **2008**, *8*, 1400–1458. [CrossRef]
144. Pillai, S.; Upadhyay, A.; Sayson, D.; Nguyen, B.H.; Tran, S.D. Advances in medical wearable biosensors: Design, fabrication and materials strategies in healthcare monitoring. *Molecules* **2021**, *27*, 165. [CrossRef]
145. Lei, Y.; Zhao, W.; Zhang, Y.; Jiang, Q.; He, J.H.; Baeumner, A.J.; Alshareef, H.N. A MXene-based wearable biosensor system for high-performance in vitro perspiration analysis. *Small* **2019**, *15*, 1901190. [CrossRef]
146. Wang, Y.; Wang, X.; Lu, W.; Yuan, Q.; Zheng, Y.; Yao, B. A thin film polyethylene terephthalate (PET) electrochemical sensor for detection of glucose in sweat. *Talanta* **2019**, *198*, 86–92. [CrossRef]
147. Zhao, J.; Lin, Y.; Wu, J.; Nyein, H.Y.Y.; Bariya, M.; Tai, L.C.; Javey, A. A fully integrated and self-powered smartwatch for continuous sweat glucose monitoring. *ACS Sens.* **2019**, *4*, 1925–1933. [CrossRef] [PubMed]
148. Lin, K.C.; Muthukumar, S.; Prasad, S. Flex-GO (Flexible graphene oxide) sensor for electrochemical monitoring lactate in low-volume passive perspired human sweat. *Talanta* **2020**, *214*, 120810. [CrossRef] [PubMed]
149. Wang, R.; Zhai, Q.; An, T.; Gong, S.; Cheng, W. Stretchable gold fiber-based wearable textile electrochemical biosensor for lactate monitoring in sweat. *Talanta* **2021**, *222*, 121484. [CrossRef] [PubMed]
150. Zhang, Q.; Jiang, D.; Xu, C.; Ge, Y.; Liu, X.; Wei, Q.; Wang, Y. Wearable electrochemical biosensor based on molecularly imprinted Ag nanowires for noninvasive monitoring lactate in human sweat. *Sens. Actuat. B Chem.* **2020**, *320*, 128325. [CrossRef]
151. Fiore, L.; Mazzaracchio, V.; Serani, A.; Fabiani, G.; Fabiani, L.; Volpe, G.; Arduini, F. Microfluidic paper-based wearable electrochemical biosensor for reliable cortisol detection in sweat. *Sens. Actua. B Chem.* **2023**, *379*, 133258. [CrossRef]
152. Mazzaracchio, V.; Fiore, L.; Nappi, S.; Marrocco, G.; Arduini, F. Medium-distance affordable, flexible and wireless epidermal sensor for pH monitoring in sweat. *Talanta* **2021**, *222*, 121502. [CrossRef] [PubMed]
153. Sharma, A.; Badea, M.; Tiwari, S.; Marty, J.L. Wearable biosensors: An alternative and practical approach in healthcare and disease monitoring. *Molecules* **2021**, *26*, 748. [CrossRef]
154. Bandodkar, A.J.; Gutruf, P.; Choi, J.; Lee, K.; Sekine, Y.; Reeder, J.T.; Rogers, J.A. Battery-free, skin-interfaced microfluidic/electronic systems for simultaneous electrochemical, colorimetric, and volumetric analysis of sweat. *Sci. Adv.* **2019**, *5*, eaav3294. [CrossRef]
155. Sekine, Y.; Kim, S.B.; Zhang, Y.; Bandodkar, A.J.; Xu, S.; Choi, J.; Rogers, J.A. A fluorometric skin-interfaced microfluidic device and smartphone imaging module for in situ quantitative analysis of sweat chemistry. *Lab Chip* **2018**, *18*, 2178–2186. [CrossRef]

156. Purohit, B.; Kumar, A.; Mahato, K.; Chandra, P. Smartphone-assisted personalized diagnostic devices and wearable sensors. *Curr. Opin. Biomed Eng.* **2020**, *13*, 42–50. [CrossRef]
157. Choi, J.; Bandodkar, A.J.; Reeder, J.T.; Ray, T.R.; Turnquist, A.; Kim, S.B.; Rogers, J.A. Soft, skin-integrated multifunctional microfluidic systems for accurate colorimetric analysis of sweat biomarkers and temperature. *ACS Sens.* **2019**, *4*, 379–388. [CrossRef] [PubMed]
158. Han, X.Y.; Chen, Z.H.; Zeng, J.Z.; Fan, Q.X.; Fang, Z.Q.; Shi, G.; Zhang, M. Inorganic–organic hybrid tongue-mimic for time-resolved luminescent noninvasive pattern and chiral recognition of thiols in biofluids toward healthcare monitoring. *ACS Appl. Mat. Inter.* **2018**, *10*, 31725–31734. [CrossRef] [PubMed]
159. Promphet, N.; Ummartyotin, S.; Ngeontae, W.; Puthongkham, P.; Rodthongkum, N. Non-invasive wearable chemical sensors in real-life applications. *Anal. Chim. Acta* **2021**, *1179*, 338643. [CrossRef]
160. Soni, A.; Jha, S.K. Smartphone based non-invasive salivary glucose biosensor. *Anal. Chim. Acta* **2017**, *996*, 54–63. [CrossRef] [PubMed]
161. Soni, A.; Surana, R.K.; Jha, S.K. Smartphone based optical biosensor for the detection of urea in saliva. *Sens. Actuat. B Chem.* **2018**, *269*, 346–353. [CrossRef]
162. Promphet, N.; Hinestroza, J.P.; Rattanawaleedirojn, P.; Soatthiyanon, N.; Siralertmukul, K.; Potiyaraj, P.; Rodthongkum, N. Cotton thread-based wearable sensor for non-invasive simultaneous diagnosis of diabetes and kidney failure. *Sens. Actuat. B Chem.* **2020**, *321*, 128549. [CrossRef]
163. Promphet, N.; Rattanawaleedirojn, P.; Siralertmukul, K.; Soatthiyanon, N.; Potiyaraj, P.; Thanawattano, C.; Rodthongkum, N. Non-invasive textile based colorimetric sensor for the simultaneous detection of sweat pH and lactate. *Talanta* **2019**, *192*, 424–430. [CrossRef]
164. Siripongpreda, T.; Siralertmukul, K.; Rodthongkum, N. Colorimetric sensor and LDI-MS detection of biogenic amines in food spoilage based on porous PLA and graphene oxide. *Food Chem.* **2020**, *329*, 127165. [CrossRef]
165. Zhang, Y.; Guo, H.; Kim, S.B.; Wu, Y.; Ostojich, D.; Park, S.H.; Rogers, J.A. Passive sweat collection and colorimetric analysis of biomarkers relevant to kidney disorders using a soft microfluidic system. *Lab Chip* **2019**, *19*, 1545–1555. [CrossRef]
166. Xu, X.Y.; Yan, B. A fluorescent wearable platform for sweat Cl^- analysis and logic smart-device fabrication based on color adjustable lanthanide MOFs. *J. Mat. Chem. C* **2018**, *6*, 1863–1869. [CrossRef]
167. Miller, P.R.; Taylor, R.M.; Tran, B.Q.; Boyd, G.; Glaros, T.; Chavez, V.H.; Polsky, R. Extraction and biomolecular analysis of dermal interstitial fluid collected with hollow microneedles. *Comm. Biol.* **2018**, *1*, 173. [CrossRef] [PubMed]
168. Wang, Y.; Wu, Y.; Lei, Y. Microneedle-based glucose monitoring: A review from sampling methods to wearable biosensors. *Biomat. Sci.* **2023**, *11*, 5727–5757. [CrossRef] [PubMed]
169. Ali, M.; Namjoshi, S.; Benson, H.A.E.; Mohammed, Y.; Kumeria, T. Dissolvable polymer microneedles for drug delivery and diagnostics. *J. Control Release* **2022**, *347*, 561–589.24. [CrossRef] [PubMed]
170. Wang, J.; Lu, Z.; Cai, R.; Zheng, H.; Yu, J.; Zhang, Y.; Gu, Z. Microneedle-based transdermal detection and sensing devices. *Lab Chip* **2023**, *23*, 869–887. [CrossRef] [PubMed]
171. Blicharz, T.M.; Gong, P.; Bunner, B.M.; Chu, L.L.; Leonard, K.M.; Wakefield, J.A.; Williams, R.E.; Dadgar, M.; Tagliabue, C.A.; El Khaja, R.; et al. Microneedle-based device for the one-step painless collection of capillary blood samples. *Nat. Biomed. Eng.* **2018**, *2*, 151–157.26. [CrossRef]
172. Kim, D.; Cao, Y.; Mariappan, D.; Bono Jr, M.S.; Hart, A.J.; Marelli, B. A microneedle technology for sampling and sensing bacteria in the food supply chain. *Adv. Funct. Mat.* **2021**, *31*, 2005370. [CrossRef]
173. Tehrani, F.; Teymourian, H.; Wuerstle, B.; Kavner, J.; Patel, R.; Furmidge, A.; Wang, J. An integrated wearable microneedle array for the continuous monitoring of multiple biomarkers in interstitial fluid. *Nat. Biomed. Eng.* **2022**, *6*, 1214–1224. [CrossRef]
174. Paul, R.; Saville, A.C.; Hansel, J.C.; Ye, Y.; Ball, C.; Williams, A.; Wei, Q. Extraction of plant DNA by microneedle patch for rapid detection of plant diseases. *ACS Nano* **2019**, *13*, 6540–6549. [CrossRef]
175. Lee, H.; Choi, T.K.; Lee, Y.B.; Cho, H.R.; Ghaffari, R.; Wang, L.; Kim, D.H. A graphene-based electrochemical device with thermoresponsive microneedles for diabetes monitoring and therapy. *Nat. Nanotechnol.* **2016**, *11*, 566–572. [CrossRef]
176. Yu, J.; Wang, J.; Zhang, Y.; Chen, G.; Mao, W.; Ye, Y.; Gu, Z. Glucose-responsive insulin patch for the regulation of blood glucose in mice and minipigs. *Nat. Biomed. Eng.* **2020**, *4*, 499–506. [CrossRef]
177. Teymourian, H.; Barfidokht, A.; Wang, J. Electrochemical glucose sensors in diabetes management: An updated review (2010–2020). *Chem. Soc. Rev.* **2020**, *49*, 7671–7709. [CrossRef]
178. Wang, L.; Xie, S.; Wang, Z.; Liu, F.; Yang, Y.; Tang, C.; Peng, H. Functionalized helical fibre bundles of carbon nanotubes as electrochemical sensors for long-term in vivo monitoring of multiple disease biomarkers. *Nat. Biomed. Eng.* **2020**, *4*, 159–171. [CrossRef]
179. Lee, H.; Hong, Y.J.; Baik, S.; Hyeon, T.; Kim, D.H. Enzyme-based glucose sensor: From invasive to wearable device. *Adv. Health Mat.* **2018**, *7*, 1701150. [CrossRef]
180. Tian, K.; Prestgard, M.; Tiwari, A. A review of recent advances in nonenzymatic glucose sensors. *Mat. Sci. Eng. C* **2014**, *41*, 100–118. [CrossRef]
181. Adeel, M.; Rahman, M.M.; Caligiuri, I.; Canzonieri, V.; Rizzolio, F.; Daniele, S. Recent advances of electrochemical and optical enzyme-free glucose sensors operating at physiological conditions. *Biosens. Bioelectron.* **2020**, *165*, 112331. [CrossRef]

182. Manasa, G.; Mascarenhas, R.J.; Shetti, N.P.; Malode, S.J.; Mishra, A.; Basu, S.; Aminabhavi, T.M. Skin patchable sensor surveillance for continuous glucose monitoring. *ACS Appl. Bio Mater.* **2022**, *5*, 945–970. [CrossRef]
183. Sharma, S.; Huang, Z.; Rogers, M.; Boutelle, M.; Cass, A.E. Evaluation of a minimally invasive glucose biosensor for continuous tissue monitoring. *Anal. Bioanal Chem.* **2016**, *408*, 8427–8435. [CrossRef]
184. Windmiller, J.R.; Valdés-Ramírez, G.; Zhou, N.; Zhou, M.; Miller, P.R.; Jin, C.; Wang, J. Bicomponent microneedle array biosensor for minimally-invasive glutamate monitoring. *Electroanal* **2011**, *23*, 2302–2309. [CrossRef]
185. Chen, D.; Wang, C.; Chen, W.; Chen, Y.; Zhang, J.X. PVDF-Nafion nanomembranes coated microneedles for in vivo transcutaneous implantable glucose sensing. *Biosens. Bioelectron.* **2015**, *74*, 1047–1052. [CrossRef]
186. Zhang, B.L.; Yang, Y.; Zhao, Z.Q.; Guo, X.D. A gold nanoparticles deposited polymer microneedle enzymatic biosensor for glucose sensing. *Electrochim. Acta* **2020**, *358*, 136917. [CrossRef]
187. Gao, J.; Huang, W.; Chen, Z.; Yi, C.; Jiang, L. Simultaneous detection of glucose, uric acid and cholesterol using flexible microneedle electrode array-based biosensor and multi-channel portable electrochemical analyzer. *Sens. Actuat. B Chem.* **2019**, *287*, 102–110. [CrossRef]
188. Liu, Y.; Yu, Q.; Luo, X.; Yang, L.; Cui, Y. Continuous monitoring of diabetes with an integrated microneedle biosensing device through 3D printing. *Microsyst. Nanoeng.* **2021**, *7*, 75. [CrossRef]
189. Teymourian, H.; Moonla, C.; Tehrani, F.; Vargas, E.; Aghavali, R.; Barfidokht, A.; Wang, J. Microneedle-based detection of ketone bodies along with glucose and lactate: Toward real-time continuous interstitial fluid monitoring of diabetic ketosis and ketoacidosis. *Anal. Chem.* **2019**, *92*, 2291–2300. [CrossRef]
190. Trzebinski, J.; Sharma, S.; Moniz, A.R.B.; Michelakis, K.; Zhang, Y.; Cass, A.E. Microfluidic device to investigate factors affecting performance in biosensors designed for transdermal applications. *Lab Chip* **2012**, *12*, 348–352. [CrossRef]
191. Valdés-Ramírez, G.; Li, Y.C.; Kim, J.; Jia, W.; Bandodkar, A.J.; Nuñez-Flores, R.; Wang, J. Microneedle-based self-powered glucose sensor. *Electrochem. Comm.* **2014**, *47*, 58–62. [CrossRef]
192. Caliò, A.; Dardano, P.; Di Palma, V.; Bevilacqua, M.F.; Di Matteo, A.; Iuele, H.; De Stefano, L. Polymeric microneedles based enzymatic electrodes for electrochemical biosensing of glucose and lactic acid. *Sens. Actuat. B Chem.* **2016**, *236*, 343–349. [CrossRef]
193. Kim, K.B.; Choi, H.; Jung, H.J.; Oh, Y.J.; Cho, C.H.; Min, J.H.; Cha, H.J. Mussel-inspired enzyme immobilization and dual real-time compensation algorithms for durable and accurate continuous glucose monitoring. *Biosens. Bioelectron.* **2019**, *143*, 111622. [CrossRef]
194. Dervisevic, M.; Alba, M.; Yan, L.; Senel, M.; Gengenbach, T.R.; Prieto-Simon, B.; Voelcker, N.H. Transdermal electrochemical monitoring of glucose via high-density silicon microneedle array patch. *Adv. Func. Mater.* **2022**, *32*, 2009850. [CrossRef]
195. Bollella, P.; Sharma, S.; Cass, A.E.; Tasca, F.; Antiochia, R. Minimally invasive glucose monitoring using a highly porous gold microneedles-based biosensor: Characterization and application in artificial interstitial fluid. *Catalysts* **2019**, *9*, 580. [CrossRef]
196. Bollella, P.; Sharma, S.; Cass, A.E.G.; Antiochia, R. Minimally-invasive microneedle-based biosensor array for simultaneous lactate and glucose monitoring in artificial interstitial fluid. *Electroanal* **2019**, *31*, 374–382. [CrossRef]
197. Kim, K.B.; Lee, W.C.; Cho, C.H.; Park, D.S.; Cho, S.J.; Shim, Y.B. Continuous glucose monitoring using a microneedle array sensor coupled with a wireless signal transmitter. *Sens. Actuat. B Chem.* **2019**, *281*, 14–21. [CrossRef]
198. Invernale, M.A.; Tang, B.C.; York, R.L.; Le, L.; Hou, D.Y.; Anderson, D.G. Microneedle electrodes toward an amperometric glucose-sensing smart patch. *Adv. Health Mater.* **2014**, *3*, 338–342. [CrossRef]
199. Dong, Q.; Ryu, H.; Lei, Y. Metal oxide based non-enzymatic electrochemical sensors for glucose detection. *Electrochim. Acta* **2021**, *370*, 137744. [CrossRef]
200. Rasheed, T.; Rizwan, K. Metal-organic frameworks based hybrid nanocomposites as state-of–the-art analytical tools for electrochemical sensing applications. *Biosens. Bioelectron.* **2022**, *199*, 113867. [CrossRef]
201. Yoon, Y.; Lee, G.S.; Yoo, K.; Lee, J.B. Fabrication of a microneedle/CNT hierarchical micro/nano surface electrochemical sensor and its in-vitro glucose sensing characterization. *Sensors* **2013**, *13*, 16672–16681. [CrossRef]
202. Lee, S.J.; Yoon, H.S.; Xuan, X.; Park, J.Y.; Paik, S.J.; Allen, M.G. A patch type non-enzymatic biosensor based on 3D SUS microneedle electrode array for minimally invasive continuous glucose monitoring. *Sens. Actuat. B Chem.* **2016**, *222*, 1144–1151. [CrossRef]
203. Chinnadayyala, S.R.; Park, I.; Cho, S. Nonenzymatic determination of glucose at near neutral pH values based on the use of nafion and platinum black coated microneedle electrode array. *Microchim. Acta* **2018**, *185*, 250. [CrossRef]
204. He, R.; Niu, Y.; Li, Z.; Li, A.; Yang, H.; Xu, F.; Li, F. A hydrogel microneedle patch for point-of-care testing based on skin interstitial fluid. *Adv. Health Mater.* **2020**, *9*, 1901201. [CrossRef]
205. Li, C.G.; Joung, H.A.; Noh, H.; Song, M.B.; Kim, M.G.; Jung, H. One-touch-activated blood multidiagnostic system using a minimally invasive hollow microneedle integrated with a paper-based sensor. *Lab Chip* **2015**, *15*, 3286–3292. [CrossRef]
206. Nicholas, D.; Logan, K.A.; Sheng, Y.; Gao, J.; Farrell, S.; Dixon, D.; Callan, J.F. Rapid paper based colorimetric detection of glucose using a hollow microneedle device. *Int. J. Pharma* **2018**, *47*, 244–249. [CrossRef]
207. Lee, H.; Bonfante, G.; Sasaki, Y.; Takama, N.; Minami, T.; Kim, B. Porous microneedles on a paper for screening test of prediabetes. *Med. Dev. Sens.* **2020**, *3*, e10109. [CrossRef]
208. Zhu, D.D.; Duong, P.K.; Cheah, R.H.; Liu, X.Y.; Wong, J.R.; Wang, W.J.; Chen, P. Colorimetric microneedle patches for multiplexed transdermal detection of metabolites. *Biosens. Bioelectron.* **2022**, *212*, 114412. [CrossRef]

209. Wang, Z.; Li, H.; Wang, J.; Chen, Z.; Chen, G.; Wen, D.; Chan, A.; Gu, Z. Transdermal colorimetric patch for hyperglycemia sensing in diabetic mice. *Biomat* **2020**, *237*, 119782. [CrossRef]
210. Hsu, W.-L.; Huang, C.-Y.; Hsu, Y.-P.; Hwang, T.-L.; Chang, S.-H.; Wang, H.-Y.J.; Feng, L.-Y.; Tzou, S.-J.; Wei, K.-C.; Yang, H.-W. On-skin glucose-biosensing and on-demand insulin-zinc hexamers delivery using microneedles for syringe-free diabetes management. *Chem. Eng. J.* **2020**, *398*, 125536. [CrossRef]
211. Zhang, X.X.; Chen, G.P.; Bian, F.K.; Cai, L.J.; Zhao, Y.J. Encoded microneedle arrays for detection of skin interstitial fluid biomarkers. *Adv. Mater.* **2019**, *31*, 1902825. [CrossRef]
212. Wang, Z.; Luan, J.; Seth, A.; Liu, L.; You, M.; Gupta, P.; Rathi, P.; Wang, Y.; Cao, S.; Jiang, Q.; et al. Microneedle patch for the ultrasensitive quantification of protein biomarkers in interstitial fluid. *Nat. Biomed. Eng.* **2021**, *5*, 64–76. [CrossRef]
213. Zheng, H.; GhavamiNejad, A.; GhavamiNejad, P.; Samarikhalaj, M.; Giacca, A.; Poudineh, M. Hydrogel microneedle-assisted assay integrating aptamer probes and fluorescence detection for reagentless biomarker quantification. *ACS Sens.* **2022**, *7*, 2387–2399. [CrossRef]
214. Sang, M.; Cho, M.; Lim, S.; Min, I.S.; Han, Y.; Lee, C.; Shin, J.; Yoon, K.; Yeo, W.-H.; Lee, T.; et al. Fluorescent-based biodegradable microneedle sensor array for tether-free continuous glucose monitoring with smartphone application. *Sci. Adv.* **2023**, *9*, 1765. [CrossRef]
215. Zou, Y.; Chu, Z.; Guo, J.; Liu, S.; Ma, X.; Guo, J. Minimally invasive electrochemical continuous glucose monitoring sensors: Recent progress and perspective. *Biosens. Bioelectron.* **2023**, *225*, 115103. [CrossRef]